

000 001 TS²: TRAINING WITH SPARSEMAX+, TESTING WITH 002 SOFTMAX FOR ACCURATE AND DIVERSE LLM FINE- 003 TUNING 004 005

006 **Anonymous authors**
007 Paper under double-blind review
008
009
010

011 ABSTRACT 012

013 Large Language Models typically rely on Supervised Fine-Tuning (SFT) with
014 Cross-Entropy (CE) loss to specialize in downstream tasks. However, CE forces
015 the distribution toward one-hot targets and ignores alternative continuations,
016 thereby limiting output diversity, a key drawback for generative applications that
017 rely on sampling-based exploration. In this paper, we propose “Training with
018 Sparsemax+, Testing with Softmax (TS²)”. Intuitively, sparsemax and its tailored
019 loss mask the gradients of probabilities outside the support set, leaving excessive
020 probability mass on irrelevant tail classes when evaluating with softmax. To ad-
021 dress this issue, we propose an improved variant, Sparsemax+, for training, which
022 augments the sparsemax loss with a suppression term that penalizes the out-of-
023 support probabilities. At testing, we decode with softmax, yielding calibrated,
024 non-degenerate probabilities where plausible near-ties survive. We fine-tuned
025 Llama-3.1-8B and Qwen-2.5-7B with TS², achieving consistent improvements
026 in accuracy and output diversity across chat, code, and open-domain benchmarks.
027 Together, these results demonstrate that TS² provides a practical, drop-in solution
028 for fine-tuning LLMs that are both more accurate and more creative.
029
030

1 INTRODUCTION

031 Supervised fine-tuning (SFT) is one of the major steps in the Large Language Models (LLMs) post-
032 training stage: with a small amount of high-quality annotated data, it teaches models to organize
033 language better and produce instruction-following responses. The default loss function is cross-
034 entropy loss, mainly because it coincides with maximum likelihood and is a strictly proper scoring
035 rule, so minimizing it recovers the data generating conditional under well-specification (Gneiting &
036 Raftery, 2007). However, the same geometry drives the probability mass toward the one-hot target
037 and away from plausible alternatives, yielding overconfident posteriors and reduced useful diversity.
038 A large body of work seeks to counteract this overconfidence and recover useful diversity. One
039 branch changes only the decoding, e.g., nucleus sampling and best-of- N , leaving training dynamics
040 and calibration untouched (Holtzman et al., 2020). Another branch alters the training signal itself.
041 The recent GEM framework reframes SFT as reverse-KL minimization with an entropy regular-
042 izer, improving variety and mitigating overfitting (Li et al., 2025). These approaches highlight a
043 fundamental issue: promoting diversity can conflict with keeping probabilities calibrated and tails
044 disciplined.

045 We argue that the field lacks a precise operational notion of useful “diversity” for instruction follow-
046 ing. In many tasks, we do not want to “spread probability” indiscriminately over the entire vocab-
047 ularly. Instead, we want probability mass concentrated among a handful of semantically plausible
048 next tokens, those with a real chance of leading to a high quality continuation, while aggressively
049 deflating the long tail of obviously incorrect tokens toward (near) zero. The right diversity is *within*
050 the *plausible set*, not across the whole simplex. The forward KL $KL(p \parallel q)$ is mean-seeking, incen-
051 tivizing probability wherever the data has support; the reverse KL $KL(q \parallel p)$ is mode-seeking, con-
052 centrating mass on promising regions (Minka, 2005). This lens helps explain why CE with entropy
053 maximization (a forward-KL-flavored objective under softmax) can inflate low-probability tokens,
while reverse-KL flavored objectives like GEM avoid gratuitous tail mass. Yet even reverse-KL does
not guarantee that clearly implausible tokens go to zero.

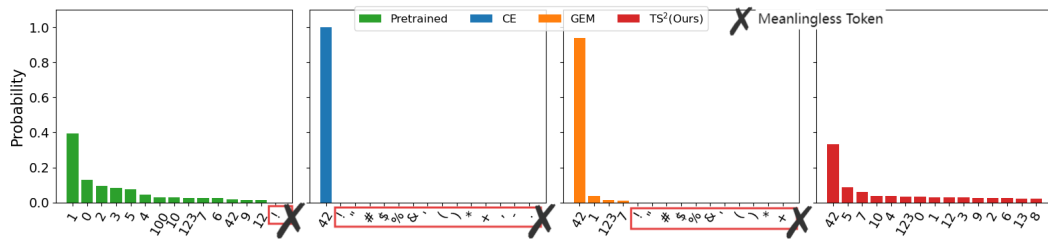


Figure 1: Token Distribution for single digit generation (detailed in Appendix C.4).

Our approach takes a geometric route by decoupling the mapping from logits to probabilities between training and testing. Specifically, we train with sparsemax and optimize a modified Fenchel–Young loss tailored to this mapping (Martins & Astudillo, 2016; Blondel et al., 2019), while at inference we revert to softmax, which restores calibrated and smooth probabilities on the same logits. Our tailored loss contains a tail penalty that drives non-support tokens to zero while ensuring the gold token is never penalized, even if it lies outside the instantaneous sparsemax support. Notably, CE with softmax collapses diversity: all non-gold logits, even plausible ones, are pushed toward zero. In contrast, sparsemax maintains a sparse support set by zeroing gradients of non-support tokens, preserving plausible candidates. However, if sparsemax were also used at inference, a converged model would still produce one-hot outputs, similar to CE with softmax decoding, thus limiting diversity (Martins & Astudillo, 2016; Blondel et al., 2019). Figure 1 shows that the pretrained model naturally exhibits diversity, but such diversity is lost during SFT: CE training drives the distribution into a one-hot solution, while GEM manages to retain only a few candidates, with most remaining probability mass assigned to irrelevant symbols. In contrast, our method delivers stronger and more stable diversity: the candidate set is both meaningful and varied, striking a balance between plausibility and coverage.

This decoupled recipe, Train with Sparsemax+, Test with Softmax (TS^2), has two key effects. During training, sparse gradients act as a principled early-stopping mechanism by avoiding wasted updates on already separated tail candidates. At inference, reverting to softmax restores smooth, calibrated probabilities so that plausible near-ties survive and sampling can explore them without aggressive temperature tuning. By construction, our method achieves local diversity among plausible tokens while assigning near-zero confidence to implausible ones. We position TS^2 among complementary strategies. Inference-only methods (e.g., nucleus, top- k , best-of- N) improve sample variety but leave training untouched; our approach reshapes training dynamics while remaining fully compatible with such decoders (Holtzman et al., 2020). Entropy targeting methods (e.g., GEM) promote spread but do not enforce exact zeros on implausible tokens; our penalty term supplies this “hard” suppression, while sparsemax ensures spread occurs where it matters (Li et al., 2025). Finally, because TS^2 decouples mappings rather than altering model architecture, it integrates seamlessly into existing SFT pipelines. The contribution of this paper are summarized in the following:

- We frame the problem as achieving Tail-Suppressed Plausible Diversity (TSPD) and propose TS^2 , which decouples training and inference by using a Sparsemax+ loss with tail penalty for training and standard softmax for decoding.
- We provide a theoretical analysis showing how TS^2 avoids the distributional collapse common to CE training via a gradient-masking mechanism, thereby preserving diversity at inference.
- We demonstrate in practice that our TS^2 significantly improves winrates, sample efficiency in code generation, and output diversity across multiple benchmarks compared to existing methods.

2 DISTRIBUTION COLLAPSE AND OUR INSIGHT

Recent studies have observed an “alignment tax” in large language models (LLMs): while supervised fine-tuning (SFT) improves faithfulness and task adherence (Brown et al., 2020), it often comes at the cost of reduced output diversity and partial forgetting of pre-trained knowledge (O’Mahony et al., 2024; Kim et al., 2025). Pre-trained LLMs naturally exhibit a broad generative repertoire, producing multiple semantically valid outputs for the same prompt (Wang et al., 2025). However, after SFT, models tend to respond with highly deterministic and homogeneous output (Li et al., 2025), weakening their utility in downstream applications such as planning (Song et al., 2023), writing (Lee

108 et al., 2022), or code generation (Liu et al., 2023), all of which fundamentally rely on the ability to
 109 explore diverse candidate responses.
 110

111 A central obstacle in supervised fine-tuning is that cross-entropy (CE), driving the predictive distribution
 112 towards a one-hot distribution, causing all probability mass to collapse onto the gold token.
 113 This *distribution collapse* ensures convergence, but comes at a severe cost: the model suppresses
 114 all alternatives to nearly zero, leading to deterministic outputs, both in the choice of tokens and in
 115 the semantic content of the whole responses. The mechanism destroys *diversity*, erasing helpful
 116 variations preserved in the pre-trained distribution and thereby yielding monotonous generations.
 117

2.1 OUR GUIDING INSIGHT: TAIL-SUPPRESSED PLAUSIBLE DIVERSITY

119 In generative modeling, output diversity is essential. A target distribution should retain a compact set
 120 of plausible candidates with non-negligible probability while suppressing irrelevant long-tail tokens
 121 toward zero. We formalize this as *Tail-Suppressed Plausible Diversity (TSPD)*, which remedies the
 122 distribution collapse commonly observed in existing SFT.
 123

124 **Notation.** We consider prompt-response pairs $(x, y) \in \mathcal{D}$ from a supervised dataset \mathcal{D} . Let f_θ
 125 denote a pre-trained LLM parameterized by θ . For a prompt x , let $\mathbf{z} = f_\theta(x) \in \mathbb{R}^K$ denote the
 126 corresponding logit vector¹. We define the probability simplex as $\Delta^{K-1} = \{\mathbf{p} \in \mathbb{R}^K \mid p_i \geq$
 127 $0, \sum_{i=1}^K p_i = 1\}$, where $\mathbf{p} = g(\mathbf{z})$ denotes a probability distribution obtained from the logits \mathbf{z} via
 128 a probability mapping function $g(\cdot)$.
 129

130 **Definition 1** (Tail-Suppressed Plausible Diversity $(m, \varepsilon_{\text{head}}, \varepsilon_{\text{tail}})$). *Given a prompt-response pair*
 131 (x, y) , *let $\mathbf{p} = g(f_\theta(x)) \in \Delta^{K-1}$ be a distribution over a vocabulary \mathcal{V} . Fix an integer $m \geq 2$ and*
 132 *thresholds $0 < \varepsilon_{\text{head}} \leq \frac{1}{m}$ and $0 \leq \varepsilon_{\text{tail}} \leq 1 - m \varepsilon_{\text{head}}$. Let $\text{Top}_m(\mathbf{p})$ denote the indices of the m*
 133 *largest coordinates of \mathbf{p} . If $y \in \text{Top}_m(\mathbf{p})$, let $\mathcal{S} := \text{Top}_m(\mathbf{p})$; otherwise, let $\mathcal{S} := \text{Top}_{m-1}(\mathbf{p}) \cup \{y\}$.*
 134 *We say that \mathbf{p} satisfies TSPD of order m if*

$$(\mathbf{Head} \text{ } \mathbf{Preservation}) \quad \min_{j \in \mathcal{S}} p_j \geq \varepsilon_{\text{head}}, \quad (1a)$$

$$(\mathbf{Tail} \text{ } \mathbf{Suppression}) \quad \sum_{j \notin \mathcal{S}} p_j \leq \varepsilon_{\text{tail}}. \quad (1b)$$

135 which ensures that candidates in \mathcal{S} retain non-negligible probability, whereas tokens outside \mathcal{S} receive
 136 essentially zero probability, thereby preserving uncertainty and transferable knowledge at inference.
 137 If one chooses $\varepsilon_{\text{head}} = 1/m$ exactly, then the strict requirement $\varepsilon_{\text{tail}} \geq 0$ forces $m\varepsilon_{\text{head}} = 1$ and $p_j = 0 \forall j \notin \mathcal{S}$; therefore, in practice one can take $\varepsilon_{\text{head}} < 1/m$ and relax $\varepsilon_{\text{tail}} > 0$.
 138

139 **Corollary 1.** *If Definition 1 holds and $\varepsilon_{\text{tail}} < \varepsilon_{\text{head}}$, then $\max_{j \notin \mathcal{S}} p_j \leq \varepsilon_{\text{tail}} < \varepsilon_{\text{head}} \leq \min_{i \in \mathcal{S}} p_i$, so each plausible sample has strictly higher probability than any tail sample.*
 140

141 **Corollary 2.** *If all probability mass collapses onto the ground-truth token, i.e., $p_y = 1$ and $p_{y'} = 0 \forall y' \neq y$, then \mathbf{p} fails to qualify the TSPD $(m(\geq 2), \varepsilon_{\text{head}}, \varepsilon_{\text{tail}})$.*
 142

143 In the next section, we motivate our method that operationalizes this principle, directly countering
 144 the diversity-reducing bias of CE loss while retaining the benefits of supervised fine-tuning.
 145

3 ACHIEVING TAIL-SUPPRESSED PLAUSIBLE DIVERSITY

146 A natural way to realize TSPD in Equation (1) is to exploit the sparsity of the sparsemax mapping
 147 $\text{sparsemax}(\mathbf{z})$ (Martins & Astudillo, 2016), which projects logits $\mathbf{z} \in \mathbb{R}^K$ onto the probability
 148 simplex Δ^{K-1} and can assign exact zeros to non-support tokens.
 149

150 Let $\mathbf{z} \in \mathbb{R}^K$ and let $z_{(1)} \geq z_{(2)} \geq \dots \geq z_{(K)}$ denote the sorted coordinates of \mathbf{z} . Define $k(\mathbf{z}) :=$
 151 $\max \{k \in \{1, \dots, K\} \mid 1 + k z_{(k)} > \sum_{j=1}^k z_{(j)}\}$, and the threshold $\tau(\mathbf{z}) = \frac{\sum_{j=1}^{k(\mathbf{z})} z_{(j)} - 1}{k(\mathbf{z})}$.
 152

153 The sparsemax probabilities are then given elementwise by
 154

$$p_i^{\text{sp}}(\mathbf{z}) = \text{sparsemax}(\mathbf{z})_i := \max\{z_i - \tau(\mathbf{z}), 0\}, \quad i = 1, \dots, K.$$

155 ¹ y and x can be sequential, where an auto-regressive formulation is used.
 156

162 The (data-dependent) support set is $S^{\text{sp}}(\mathbf{z}) = \{i \in \{1, \dots, K\} : p_i^{\text{sp}}(\mathbf{z}) > 0\}$, which follows from
 163 the definition above and no circularity arises. Equivalently, in vector form, $\mathbf{p}^{\text{sp}}(\mathbf{z}) = [\mathbf{z} - \tau(\mathbf{z})\mathbf{1}]_+$,
 164 where $[\mathbf{v}]_+ := \max\{\mathbf{v}, 0\}$ is applied elementwise.
 165

166 In effect, sparsemax automatically identifies a compact support set of plausible candidates $S^{\text{sp}}(\mathbf{z})$
 167 and prunes away the long tail. Compared to the softmax probability mapping $\mathbf{p}^{\text{sf}}(\mathbf{z}) =$
 168 $\frac{\exp(\mathbf{z})}{\sum_{i=1}^K \exp(z_i)} := \text{softmax}(\mathbf{z})$, its Jacobian is sparse; in particular, gradients vanish outside $S^{\text{sp}}(\mathbf{z})$
 169 when the target lies in the support (Lemma 3).
 170

171 **Lemma 3** (Gradients vanish outside the sparsemax support). (Martins & Astudillo, 2016) Let
 172 $\mathbf{p} = \text{sparsemax}(\mathbf{z})$ and $S^{\text{sp}}(\mathbf{z})$ be its support. Define $\mathcal{L}(\mathbf{p}, \mathbf{y})$ as a supervised loss between the
 173 sparsemax probability \mathbf{p} and the target \mathbf{y} . If $y \in S^{\text{sp}}(\mathbf{z})$, then $\forall i \notin S^{\text{sp}}(\mathbf{z})$, $\frac{\partial \mathcal{L}(\mathbf{z}, \mathbf{y})}{\partial z_i} = 0$.
 174

175 While sparsemax provides margin-induced sparsity, it nonetheless tends to collapse into a nearly
 176 one-hot distribution once the leading logit surpasses the margin threshold. Such collapse inevitably
 177 reduces sampling diversity, making sparsemax undesirable for inference.
 178

179 This motivates us to instead carry out decoding with softmax. Under this choice, the gradient-
 180 vanishing property established in Lemma 3 remains advantageous during training: by nullifying gra-
 181 dients outside the active support whenever the target is included, it mitigates the cross-entropy-style
 182 erosion of plausible near-optimal alternatives, thereby inducing an implicit early-stopping effect.
 183

184 **Theorem 4** (Sparsemax expands pairwise gaps faster than softmax). Let $\mathbf{z} \in \mathbb{R}^K$, $\mathbf{p}^{\text{sf}} =$
 185 $\text{softmax}(\mathbf{z})$, and $\mathbf{p}^{\text{sp}} = \text{sparsemax}(\mathbf{z})$. For any indices $i \neq j$, let $u := z_i - z_j$ and we have
 186

$$\begin{aligned} \frac{\partial}{\partial u} (p_i^{\text{sp}} - p_j^{\text{sp}}) &= 1 \quad \forall i, j \in S^{\text{sp}}, & \text{sparsemax} \\ \frac{\partial}{\partial u} (p_i^{\text{sf}} - p_j^{\text{sf}}) &< 1, & \text{softmax} \end{aligned}$$

187 Given the same logits, Theorem 4 shows that sparsemax linearly preserves pairwise probability
 188 gaps within its active support and collapses to a one-hot prediction once a finite margin is attained,
 189 whereas softmax strictly contracts such gaps. Consequently, sparsemax induces sharp discrimination
 190 and faster label collapse during training, while applying softmax to the same logits at inference
 191 preserves non-degenerate mass on plausible candidates, maintaining output diversity that is desirable
 192 for generative tasks.
 193

194 **Corollary 5** (Softmax remains TSPD-valid when sparsemax is one-hot). Let $\mathbf{z} \in \mathbb{R}^K$ with $y =$
 195 $\arg \max_j z_j$, and $\delta_j := z_y - z_j$. Assume sparsemax is one-hot at y , i.e., $\delta_{\min} := \min_{j \neq y} \delta_j \geq \gamma > 0$
 196 (e.g., $\gamma = 1$), and the top- m head is bounded: $\delta_{(k)} := z_c - z_{(k)} \leq B \quad \forall k = 2, \dots, m$. Set
 197 $A_m = m + (K - m)e^{-\gamma}$. Then for $\mathbf{p}^{\text{sf}} = \text{softmax}(\mathbf{z})$ we have
 198

$$p_y^{\text{sf}} \geq \frac{1}{A_m}, \quad p_{(k)}^{\text{sf}} \geq \frac{e^{-B}}{A_m} \quad (\forall k = 2, \dots, m), \quad \sum_{k>m} p_{(k)}^{\text{sf}} \leq \frac{(K - m)e^{-\gamma}}{A_m}.$$

199 Consequently, \mathbf{p}^{sf} satisfies TSPD of order m with any thresholds $0 < \varepsilon_{\text{head}} \leq \frac{e^{-B}}{A_m}$, $\frac{(K - m)e^{-\gamma}}{A_m} \leq$
 200 $\varepsilon_{\text{tail}} < 1 - m \varepsilon_{\text{head}}$.
 201

202 **Remark 1.** Without the head bound $\delta_{(k)} \leq B$ ($\forall k \leq m$), $p_{(m)}^{\text{sf}}$ can be made arbitrarily small even
 203 when $\delta_{\min} \geq 1$, so only a vanishingly small head floor $\varepsilon_{\text{head}}$ can be guaranteed for general m .
 204

205 **Remark 2.** [Existence of a tight upper bound for the cumulated tail mass $\sum_{k>m} p_{(k)}^{\text{sf}}$ in Corol-
 206 lary 5] Under the assumption of Corollary 5, let $\Omega_{\min} = 1 + (m - 1)e^{-B} + (K - m)e^{-\gamma}$, then we
 207 have $\sum_{k>m} p_{(k)}^{\text{sf}} \leq \frac{(K - m)e^{-\gamma}}{\Omega_{\min}}$. With the new upper bound, \mathbf{p}^{sf} still satisfies TSPD of order m with
 208 any thresholds $0 < \varepsilon_{\text{head}} \leq \frac{e^{-B}}{A_m}$, $\frac{(K - m)e^{-\gamma}}{\Omega_{\min}} \leq \varepsilon_{\text{tail}} \leq 1 - m \varepsilon_{\text{head}}$. (see Appendix D for detailed
 209 derivation.).
 210

211 According to Remark 2, the upper bound on the cumulated tail mass $\sum_{k>m} p_{(k)}^{\text{sf}}$ is strictly increasing
 212 in K and approaches 1 as $K \rightarrow \infty$. Importantly, this bound is tight (see Proposition 6 in
 213 Appendix D): there exists a worst-case configuration where the tail mass grows monotonically with
 214

216 *K*. Thus, for large vocabularies, the admissible tail under softmax at inference becomes nearly 1,
 217 indicating that sparsemax training has not theoretically guaranteed the suppression of irrelevant tail
 218 mass, contradicting the goal of suppressing irrelevant tail mass.

219 To address these issues, we propose a fine-tuning strategy of **Training with Sparsemax+, Testing**
 220 **with Softmax**. Sparsemax+ builds on Sparsemax, inheriting margin-induced sparsity to introduce
 221 gradient masking during training, thereby implicitly enforcing an early-stopping effect once the
 222 top-1 candidate is clearly separated. It further incorporates a lightweight *Tail-suppressing Loss* to
 223 explicitly penalize residual probability on tail tokens, ensuring that tail mass is sharply suppressed.
 224 At inference, we revert to softmax over the same logits, which restores smooth, calibrated proba-
 225 bilities across the plausible candidates within the support set, while keeping the irrelevant tail mass
 226 negligible due to the additional suppressing effect. In this way, the model learns to *separate and*
 227 *prune* the logits during training, yet *preserve and diversify* the output distribution during inference,
 228 achieving the desired support-aware diversity.

230 4 TS^2 : TRAINING WITH SPARSEMAX+, TESTING WITH SOFTMAX

232 In the following, we present supervised fine-tuning based on the Fenchel-Young loss, which encom-
 233 passes both the softmax and sparsemax mappings. It then motivates our Sparsemax+ loss.

235 4.1 DIFFERENT PREDICTION MAPPINGS WITH THE UNIFIED FENCHEL-YOUNG LOSS

237 For any strictly convex regularization function $\Omega : \Delta^{K-1} \rightarrow \mathbb{R}$, the corresponding regularized
 238 prediction function is $\mathbf{p}_*(\mathbf{z}) = \arg \max_{\mathbf{p} \in \Delta^{K-1}} \langle \mathbf{p}, \mathbf{z} \rangle - \Omega(\mathbf{p})$. The associated Fenchel-Young loss
 239 can be represented as

$$240 L_\Omega(\mathbf{z}; y) = \Omega(\mathbf{e}_y) - \Omega(\mathbf{p}_*) + \langle \mathbf{z}, \mathbf{p}_* - \mathbf{e}_y \rangle, \quad (3)$$

241 where y is the gold label and \mathbf{e}_y is the corresponding one-hot vector. Different choices of Ω yield
 242 different prediction mappings and losses.

243 **Softmax** Softmax corresponds to using the negative Shannon entropy as regularizer $\Omega(\mathbf{p}) =$
 244 $\sum_{i=1}^K p_i \log p_i$, which gives $\mathbf{p}_*(\mathbf{z}) = \frac{\exp(\mathbf{z})}{\sum_{i=1}^K \exp(z_i)} := \text{softmax}(\mathbf{z})$. The Fenchel-Young loss re-
 245 duces to the standard CE loss $L_{\text{softmax}}(\mathbf{z}; y) = \log \sum_{i=1}^K \exp(z_i) - z_y = -\log \frac{\exp(z_y)}{\sum_{i=1}^K \exp(z_i)}$.

247 **Sparsemax** Sparsemax corresponds to using the negative Gini entropy as regularizer $\Omega(\mathbf{p}) =$
 248 $\frac{1}{2} \sum_{i=1}^K p_i(1 - p_i)$, which gives $\mathbf{p}_*(\mathbf{z}) = [\mathbf{z} - \tau(\mathbf{z})\mathbf{1}]_+ := \text{sparsemax}(\mathbf{z})$. The cor-
 249 responding Fenchel-Young loss, called the sparsemax loss, is $L_{\text{sparsemax}}(\mathbf{z}; y) = -z_y +$
 250 $\frac{1}{2} \sum_{j \in S^{\text{sp}}(\mathbf{z})} (z_j^2 - \tau^2(\mathbf{z})) + \frac{1}{2}$.

252 In conclusion, when training with sparsemax but performing inference with softmax, although
 253 softmax(\mathbf{z}) does not yield a one-hot output like sparsemax(\mathbf{z}), it still assigns the highest probabili-
 254 ty to the correct class. Importantly, it naturally enables early stopping and preserves distributional
 255 diversity across all classes, which is consistent with the goal of diversifying plausible candidates.

256 Given prompt-response pairs (x, y) from a supervised dataset, let $\mathbf{z} \in \mathbb{R}^K$ be a logit vector and
 257 \mathbf{p} be probability mapping either via softmax or sparsemax. If the gradient of the sparsemax loss
 258 vanishes, i.e., $\nabla_{\mathbf{z}} \mathcal{L}_{\text{sparsemax}}(\mathbf{z}; y) = 0$, then it follows that $\text{sparsemax}(\mathbf{z})_y = 1$. For any index
 259 $\forall j \neq y$, $\text{sparsemax}(\mathbf{z})_j = 0$, it holds that $\text{softmax}(\mathbf{z})_j > 0$. That is, softmax assigns non-zero
 260 probability to all entries, including those which sparsemax maps to zero. According to Corollary 5,
 261 the cumulated tail mass of softmax outside the top- m satisfies $\sum_{k>m} p_{(k)}^{\text{sf}} \leq \frac{(K-m)e^{-\gamma}}{A_m}$. With
 262 large vocabularies, the admissible tail under softmax at inference becomes nearly 1. This behavior
 263 is undesirable, as assigning non-negligible probabilities to clearly incorrect classes may lead the
 264 model to produce semantically meaningless outputs.

265 **Sparsemax+** To address this issue, we introduce a lightweight tail-suppressing loss that explicitly
 266 suppresses probabilities assigned to the non-plausible candidates. Given logits $\mathbf{z} \in \mathbb{R}^K$, let $\mathbf{p}^{\text{sf}} =$
 267 $\text{softmax}(\mathbf{z}) \in \Delta^{K-1}$. The tail-suppressing loss is defined as

$$269 \mathcal{L}_{\text{sup}}(\mathbf{p}; y) = -\log(1 - \sum_{i \notin \mathcal{S}} p_i^{\text{sf}}),$$

270 **Algorithm 1** TS^2 : Training with Sparsemax+, Testing with Softmax

271 **Input:** pre-trained model f_θ ; training dataset $\mathcal{D}_{tr} = \{(x, y)\}$; test dataset $\mathcal{D}_{te} = \{x\}$.

272 **Hyperparameters:** epochs T ; batch size B ; learning rate $\eta > 0$; suppression weight $\alpha > 0$.

273 1: **for** $t = 1$ to T **do** ▷ Training Phase

274 2: **for** mini-batch $\{(\mathbf{x}_b, \mathbf{y}_b)\}_{b=1}^B \subset \mathcal{D}_{tr}$ **do**

275 3: Compute logits $\mathbf{z}_b \leftarrow f_\theta(\mathbf{x}_b)$, $\forall b = 1, 2, \dots, B$

276 4: Compute loss $L_b \leftarrow L_{\text{spm}^+}(\mathbf{z}_b; \mathbf{y}_b)$, $\forall b = 1, 2, \dots, B$ ▷ Sparsemax+ loss

277 5: **end for**

278 6: Update $\theta \leftarrow \theta - \eta \nabla_\theta \frac{1}{B} \sum_{b=1}^B L_b$

279 7: **end for**

280 8: **for** test input $\mathbf{x} \in \mathcal{D}_{te}$ **do** ▷ Testing Phase

281 9: Compute logits $\mathbf{z} \leftarrow f_\theta(\mathbf{x})$

282 10: Predict probability $\mathbf{p} \leftarrow \text{softmax}(\mathbf{z})$

283 11: Evaluation on \mathbf{p} ▷ Use for decoding

284 12: **end for**

285

286 where \mathcal{S} is defined in Definition 1. This penalty drives the probabilities of tail tokens toward zero, thereby avoiding residual mass on clearly implausible candidates.

287 **Remark 3.** *The tail suppressing loss can be interpreted as a direct generalization of the standard softmax CE to the group-label setting. Specifically, given logits \mathbf{z} and softmax distribution $\mathbf{p}^{\text{sf}} = \text{softmax}(\mathbf{z})$, the suppressing term can be written as*

$$288 \quad L_{\text{sup}}(\mathbf{z}) = -\log(1 - \sum_{i \notin \mathcal{S}} p_i^{\text{sf}}) = -\log \sum_{i \in \mathcal{S}} p_i^{\text{sf}},$$

289 which is exactly the softmax cross-entropy with the target label being the merged “super-class” \mathcal{S} .
290 In the special case where $\mathcal{S} = \{y\}$ is a singleton, this reduces to the usual CE loss $-\log p_y^{\text{sf}}$. Thus,
291 the suppressing loss can be viewed as encouraging the softmax probability mass to concentrate on
292 a set of plausible candidates while retaining the probabilistic interpretation of cross-entropy.

293 Combining sparsemax with the tail-suppressing loss yields our proposed *Sparsemax+ loss*:

$$294 \quad L_{\text{spm}^+}(\mathbf{z}; y) = -z_y + \frac{1}{2} \sum_{j \in S^{\text{sp}}(\mathbf{z})} (z_j^2 - \tau^2(\mathbf{z})) + \alpha \left(-\log \left(1 - \sum_{i \notin S^{\text{sp}}(\mathbf{z}), i \neq y} p_i^{\text{sf}} \right) \right), \quad (4)$$

295 where $\tau(\mathbf{z})$ is the sparsemax threshold and $\alpha > 0$ controls the strength of the suppression. For sim-
296 plicity, we find that directly implementing the candidate set \mathcal{S} from Definition 1 using the sparsemax
297 support $S^{\text{sp}}(\mathbf{z})$ achieves superior performance.

298 We summarize our fine-tuning strategy of **Training with Sparsemax+, Testing with Softmax** in
299 Algorithm 1. From $L_{\text{spm}^+}(\mathbf{z}; y)$ in equation 4, we see that it prevents CE-style erosion of plausible
300 near-ties by amplifying relative ratios among top logits while nulling the rest, thereby achieving two
301 goals: sparsemax selects a stable support set with early stopping of gradient flow, and the suppress-
302 ing term explicitly drives unreasonable tokens toward zero to prevent spurious mass at inference.

312 5 EXPERIMENTS

313 To situate our work within the current state-of-the-art, we build upon the experimental foundation of
314 GEM (Li et al., 2025), adopting a similar training setup. Our primary methodological difference is
315 the substitution of the GEM objective with our proposed TS^2 loss. Furthermore, while GEM eval-
316 uates OpenLLM Leaderboard tasks using a standard one shot setting, we employ a multi-response,
317 best-of-N protocol. We argue this is a more faithful and informative evaluation for diversity aware
318 models, as it measures model’s latent ability to find the correct answer rather than penalizing it for
319 plausible “hesitation” in a single attempt.

320 **Setup.** We conduct experiments on two powerful, open source base models: Llama-3.1-8B and
321 Qwen-2-7B. For supervised finetuning, we use the high quality UltraFeedback dataset (Cui
322 et al., 2024), a large-scale corpus of preference aligned responses generated by a diverse set of

models. All models are finetuned for 3 epochs using the AdamW optimizer with an effective batch size of 128. We employ a cosine learning rate schedule with an initial rate of 2×10^{-5} and a warm-up ratio of 0.03, a standard practice for fine-tuning modern LLMs (Yu et al., 2024; Liu et al., 2024). The maximum sequence length is capped at 2,048 tokens. For our proposed TS^2 method, the suppression weight α (see Equation 4) is empirically determined for each model architecture, with optimal values reported alongside results. Further implementation details are provided in the Appendix B.

We compare TS^2 against a suite of strong and relevant baselines to provide a comprehensive evaluation: **Cross-entropy (CE)**: The standard SFT objective, which serves as our primary baseline. **CE with Weight Decay (CE+WD)**: A common regularization technique shown to help preserve diversity in instruction tuning (Ouyang et al., 2022; Bai et al., 2022). We use a weight decay coefficient of 0.1. **NEFTune (NEFT)**: A regularization method that adds noise to word embeddings during training to mitigate overfitting and improve generalization (Jain et al., 2023). **GEM**: The current state-of-the-art method for diversity preserving SFT, which we use as our main point of comparison (Li et al., 2025).

5.1 IMPROVING ACCURACY AND DIVERSITY IN OPEN-ENDED GENERATION

We first evaluate TS^2 in open ended domains to assess its ability to navigate the critical trade-off between response quality and diversity. While standard fine-tuning often improves quality at the cost of collapsing the output distribution, we hypothesize that TS^2 can break this trade-off by simultaneously enhancing generation quality and fostering a rich, useful diversity beneficial for sampling-based decoding. To test this, we evaluate on two distinct benchmarks. For conversational chat, we use the AlpacaEval dataset (Dubois et al., 2024) with a best-of-32 (BoN@32) protocol; a state-of-the-art reward model, FsfairX-LLaMA3-RM-v0.1 (Lambert et al., 2024), selects the best response, which is then compared against GPT-4 to determine a win rate. For code generation, we measure the pass@k metric on the HumanEvalbenchmark (Chen et al., 2021), which assesses the model’s ability to generate functionally correct Python code via execution.

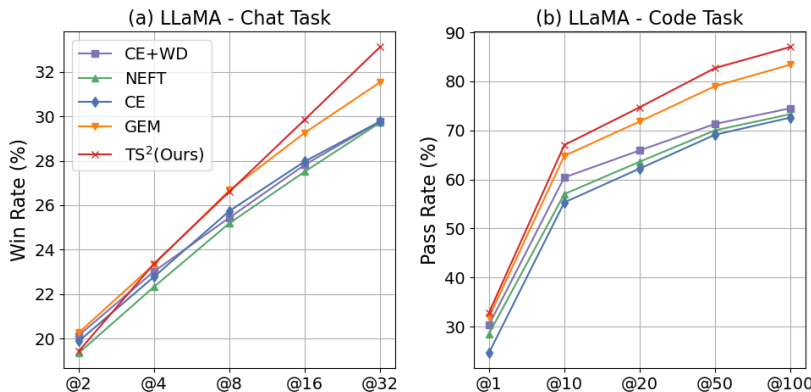


Figure 2: Performance of Llama-3.1-8B on open-ended tasks. Left: Win rate on AlpacaEval vs. sampling budget (N). Right: Pass rate on HumanEval vs. sampling budget (k). TS^2 consistently outperforms baselines.

Performance on Chat and Code Generation. As shown in Figure 2, TS^2 demonstrates a clear performance advantage on Llama-3.1-8B. In chat generation, its win rate at a budget of N=32 responses, reaches 33.12%, which is an improvement of 11.2% relative over the baseline cross entropy loss and a 5.0% relative improvement over the strong GEM baseline. This advantage extends to structured problem solving, on HumanEval, TS^2 achieves a pass@100 of 87.00%, which is 4.3% increase relative to GEM and 19.8% to that of CE. Notably, the diversity fostered by our method translates to superior sample efficiency: the pass@50 rate for TS^2 (82.70%) nearly matches GEM’s pass@100 performance (83.40%), indicating that correct solutions can be found with fewer samples. Similar results are also observed for Qwen-2-7B model. Detailed breakdown of results for both Llama-3.1-8B and Qwen-2-7B are detailed in the Table 8.

Model	Method	Win Rate (%) ↑	N-gram ↑	100 - Self-BLEU ↑	Sent-BERT ↑
LLaMA-3.1-8B	CE	29.77	17.78	47.04	9.97
	CE+WD	29.72	17.78	47.14	10.03
	NEFT	29.77	17.74	47.41	10.07
	GEM	31.53	20.32	49.82	11.16
	TS² (Ours)	33.12	23.78	53.87	12.80
Qwen-2-7B	CE	31.41	17.23	16.77	7.95
	CE+WD	31.05	17.43	17.08	8.06
	NEFT	30.36	16.59	24.59	8.06
	GEM	33.89	24.35	31.19	9.25
	TS² (Ours)	37.48	30.15	39.04	9.81

Table 1: Win rate (Best of N@32) and diversity metrics for Llama-3.1-8B and Qwen-2-7B on AlpacaEval. TS² achieves the best results across both quality and diversity on both architectures.

Crucially, these performance gains do not come at the cost of diversity. As detailed in Table 1, TS² not only achieves the highest win rate but also scores best across all three diversity metrics. It improves N-gram diversity by 17.0%, BLEU diversity by 8.1% and sentence-bert diversity by 10.7% over GEM for Llama-3.1-8B. Similarly for Qwen-2-7B, the same metrics are improved by 23.8%, 25.1% and 6% respectively over GEM. This result confirms that TS² successfully breaks the quality-diversity trade-off, producing responses that are simultaneously judged as higher quality by a reward model while being measurably more varied.

5.1.1 DIVERSITY ON CREATIVE WRITING TASKS

To further probe the nature of the diversity generated by TS², we evaluate it on purely creative tasks: generating poems from 573 titles in the poetry8 dataset and stories from 500 prompts from ROCStories (Mostafazadeh et al., 2016). As shown in Table 2, TS² once again achieves the highest scores across all three diversity metrics on both tasks, confirming its ability to produce a wider range of high-quality, creative outputs compared to all baselines.

Method	Poem			Story		
	N-gram ↑	100 - Self-BLEU ↑	Sent-BERT ↑	N-gram ↑	100 - Self-BLEU ↑	Sent-BERT ↑
CE	38.87	55.38	14.83	44.47	67.20	22.15
CE+WD	38.92	55.69	14.17	44.43	67.26	22.22
NEFT	38.80	55.68	14.13	44.31	67.21	22.04
GEM	46.59	57.50	14.70	50.05	69.15	24.02
TS² (Ours)	49.70	59.41	16.52	52.10	70.36	24.98

Table 2: Diversity evaluation on creative writing tasks for Llama-3.1-8B. Higher is better.

5.2 PRESERVING PRE-TRAINED CAPABILITIES ON STANDARD BENCHMARKS

To assess generalization and knowledge retention, we evaluate models on six tasks from the Open-LLM Leaderboard: ARC, GSM8K, HellaSwag, MMLU, TruthfulQA, and Winogrande. Instead of the standard greedy one-shot decoding that penalizes models preserving multiple reasoning paths, we propose a best-of-n (BoN) strategy on the OpenLLM leaderboard, which is better aligned with evaluating the capabilities of diversity-preserving models.

We argue that a more faithful metric is Best-of-N (BoN) accuracy. This protocol measures the model’s latent ability to identify the correct answer within a small sampling budget, which better reflects the true underlying capabilities of a well-calibrated, diverse model. For fair comparison, all methods are evaluated under the same BoN protocol and we report the average accuracy across all tasks.

Figure 3 validates this hypothesis. While all methods are competitive at a small sampling budget, TS²’s performance scales significantly better as ‘N’(responses) increases. On Llama-3.1-8B, the average accuracy of TS² at N=32 reaches 88.88%, a massive 13.2-point absolute (+17.4% relative)

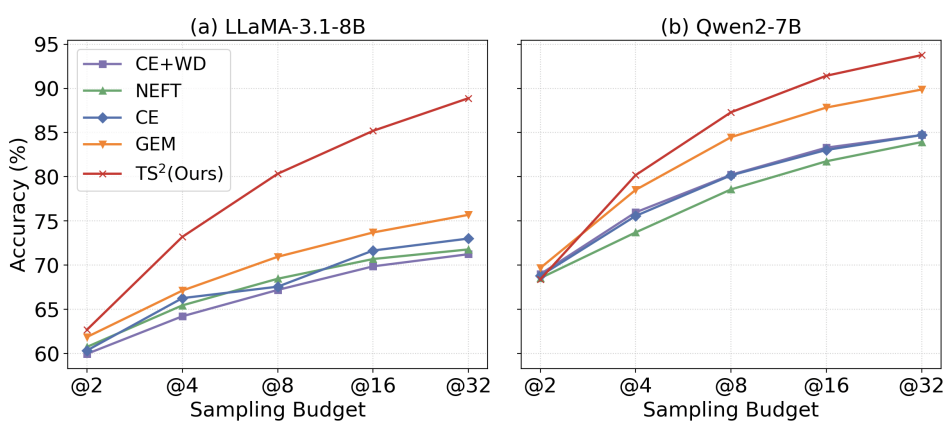


Figure 3: Average Best-of-N accuracy across six OpenLLM Leaderboard tasks. While competitive in few-shot settings (@2), TS^2 ’s performance scales far more effectively with the sampling budget, revealing its superior knowledge retention.

improvement over GEM (75.69%). The trend is consistent on Qwen-2-7B, where TS^2 again achieves the highest accuracy, demonstrating the robustness of our TS^2 across different model architectures.

This shows that TS^2 effectively preserves the model’s pre-trained knowledge. Unlike CE, which collapses the distribution and discards valid alternatives, TS^2 maintains a clean, calibrated set of high-quality reasoning paths. With sampled responses, the model consistently finds the correct solution. A detailed breakdown of performance on each of the six tasks is provided in the Table 10.

5.3 ABLATION STUDY

To assess the contribution of each component, we run an ablation study on AlpacaEval, comparing win rate against GPT-4 and BLEU diversity. TS^2 integrates three elements: (1) sparsemax-based training, (2) softmax decoding, and (3) a tail-suppression penalty. We evaluate three variants: **Decoupling Only** (sparsemax training, softmax inference, no penalty), **Unified Sparsemax** (sparsemax for both training and inference), and **Suppression Only** (CE loss with suppression term).

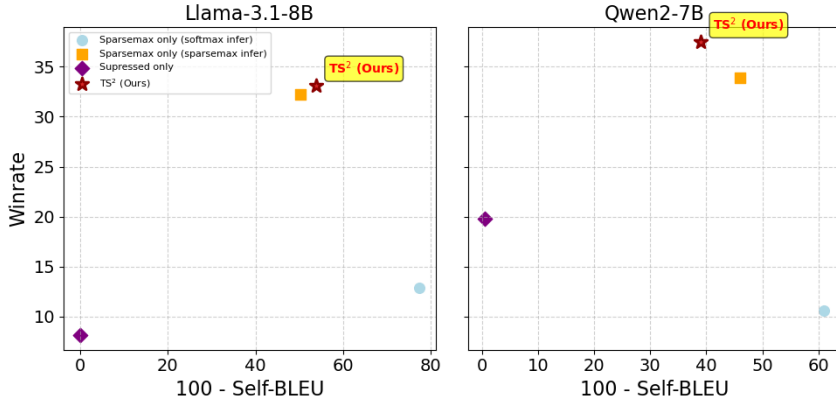


Figure 4: Ablation study on Llama-3.1-8B and Qwen2-7B.

Figure 4 demonstrates that all components of TS^2 are essential. First, using the Decoupling Only strategy results in a massive increase in diversity, high BLEU diversity score, but a catastrophic drop in win rate. This shows that while decoupling unlocks variety, the suppression penalty is crucial for ensuring that this diversity is high-quality and not just uncalibrated noise.

Conversely, the Unified Sparsemax approach achieves a competitive win rate but offers lesser diversity than our full method. This confirms that the switch to softmax at inference is key to translating the learned logit geometry into a rich, sample-able probability distribution. Finally, applying the Suppression Only penalty to a standard CE baseline fails on both metrics, proving it is not a standalone improvement but works in synergy with the sparsemax-defined support set.

486 Meanwhile, the TS^2 method successfully integrates these components, achieving the best balance
 487 of high win rate and high diversity across both model architectures. This analysis confirms that
 488 the sparsemax objective, the decoupled inference, and the suppression penalty are all necessary and
 489 synergistic elements of our approach.
 490

491 6 CONCLUSION

492
 493 In this work, we make the first step toward decoupling training and inference by adopting different
 494 prediction mappings in supervised finetuning. By combining **Sparsemax+ loss**; a tailored design
 495 that leverages margin induced sparsity with an additional suppression term for non plausible tokens;
 496 with softmax decoding at inference, our approach achieves significant improvements over existing
 497 SFT paradigms. It preserves support-aware diversity while maintaining high accuracy, thereby al-
 498 leviating the alignment tax. Despite its simplicity, our method consistently outperforms CE and
 499 GEM across both chat and code tasks, achieving the highest win rates and more diverse generations.
 500 Unlike prior methods that inevitably trade off diversity against accuracy, our paradigm improves
 501 both, providing a natural remedy to distribution collapse and open up new directions for advancing
 502 alignment with broad and long term impact.
 503

504 ETHICS STATEMENT

505
 506 This work investigates new algorithms for supervised fine-tuning of large language models. Our
 507 objective is to improve training stability and output diversity, thereby broadening the range of down-
 508 stream applications. The methods introduced in this paper are purely algorithmic and evaluated on
 509 public datasets.
 510

511 512 REPRODUCIBILITY STATEMENT

513
 514 Experiment details for reproducing our numerical results can be found in Appendix B and Ap-
 515 pendix C. To ensure anonymity and prevent potential information leakage during the review process,
 516 our source code will be released publicly after the blind review phase.
 517

518 519 LLM USAGE STATEMENT

520
 521 We used large language model to correct grammar errors, polish the writing, and adjust the format-
 522 ting of the paper.
 523

524 REFERENCES

525 Yuntao Bai, Andy Jones, Kamal Ndousse, Amanda Askell, Anna Chen, Nova DasSarma, Dawn
 526 Drain, Stanislav Fort, Deep Ganguli, Tom Henighan, Nicholas Joseph, Saurav Kadavath, Jackson
 527 Kernion, Tom Conerly, Sheer El-Showk, Nelson Elhage, Zac Hatfield-Dodds, Danny Hernan-
 528 dez, Tristan Hume, Scott Johnston, Shauna Kravec, Liane Lovitt, Neel Nanda, Catherine Olsson,
 529 Dario Amodei, Tom Brown, Jack Clark, Sam McCandlish, Chris Olah, Ben Mann, and Jared Ka-
 530 plan. Training a helpful and harmless assistant with reinforcement learning from human feedback,
 531 2022. URL <https://arxiv.org/abs/2204.05862>.

532 Mathieu Blondel, André F. T. Martins, and Vlad Niculae. Learning classifiers with fenchel–young
 533 losses: Generalized entropies, margins, and algorithms. In *Proceedings of the Twenty-Second*
 534 *International Conference on Artificial Intelligence and Statistics*, volume 89 of *Proceedings of*
 535 *Machine Learning Research*, pp. 606–615. PMLR, 2019. URL <https://proceedings.mlr.press/v89/blondel19a.html>.

536
 537 Tom Brown, Benjamin Mann, Nick Ryder, Melanie Subbiah, Jared D Kaplan, Prafulla Dhariwal,
 538 Arvind Neelakantan, Pranav Shyam, Girish Sastry, Amanda Askell, et al. Language models are
 539 few-shot learners. *Advances in neural information processing systems*, 33:1877–1901, 2020.

540 Mark Chen, Jerry Tworek, Heewoo Jun, Qiming Yuan, Henrique Ponde de Oliveira Pinto, Jared
 541 Kaplan, Harri Edwards, Yuri Burda, Nicholas Joseph, Greg Brockman, Alex Ray, Raul Puri,
 542 Gretchen Krueger, Michael Petrov, Heidy Khlaaf, Girish Sastry, Pamela Mishkin, Brooke Chan,
 543 Scott Gray, Nick Ryder, Mikhail Pavlov, Alethea Power, Lukasz Kaiser, Mohammad Bavarian,
 544 Clemens Winter, Philippe Tillet, Felipe Petroski Such, Dave Cummings, Matthias Plappert, Fotios
 545 Chantzis, Elizabeth Barnes, Ariel Herbert-Voss, William Hebgen Guss, Alex Nichol, Alex
 546 Paino, Nikolas Tezak, Jie Tang, Igor Babuschkin, Suchir Balaji, Shantanu Jain, William Saunders,
 547 Christopher Hesse, Andrew N. Carr, Jan Leike, Josh Achiam, Vedant Misra, Evan Morikawa, Alec
 548 Radford, Matthew Knight, Miles Brundage, Mira Murati, Katie Mayer, Peter Welinder, Bob Mc-
 549 Grew, Dario Amodei, Sam McCandlish, Ilya Sutskever, and Wojciech Zaremba. Evaluating large
 550 language models trained on code, 2021. URL <https://arxiv.org/abs/2107.03374>.

551 Ganqu Cui, Lifan Yuan, Ning Ding, Guanming Yao, Bingxiang He, Wei Zhu, Yuan Ni, Guotong Xie,
 552 Ruobing Xie, Yankai Lin, Zhiyuan Liu, and Maosong Sun. Ultrafeedback: Boosting language
 553 models with scaled ai feedback, 2024. URL <https://arxiv.org/abs/2310.01377>.

554 Yann Dubois, Xuechen Li, Rohan Taori, Tianyi Zhang, Ishaan Gulrajani, Jimmy Ba, Carlos
 555 Guestrin, Percy Liang, and Tatsunori B. Hashimoto. Alpacafarm: A simulation framework for
 556 methods that learn from human feedback, 2024. URL <https://arxiv.org/abs/2305.14387>.

557 Tilmann Gneiting and Adrian E. Raftery. Strictly proper scoring rules, prediction, and estimation.
 558 *Journal of the American Statistical Association*, 102(477):359–378, 2007. doi: 10.1198/
 559 016214506000001437.

560 Chuan Guo, Geoff Pleiss, Yu Sun, and Kilian Q. Weinberger. On calibration of modern neural
 561 networks. In *Proceedings of the 34th International Conference on Machine Learning*, volume 70
 562 of *Proceedings of Machine Learning Research*, pp. 1321–1330. PMLR, 2017.

563 Ari Holtzman, Jan Buys, Li Du, Maxwell Forbes, and Yejin Choi. The curious case of neural text
 564 degeneration. In *International Conference on Learning Representations*, 2020. URL <https://openreview.net/forum?id=rygGQyrFvH>.

565 Neel Jain, Ping yeh Chiang, Yuxin Wen, John Kirchenbauer, Hong-Min Chu, Gowthami Somepalli,
 566 Brian R. Bartoldson, Bhavya Kailkhura, Avi Schwarzschild, Aniruddha Saha, Micah Goldblum,
 567 Jonas Geiping, and Tom Goldstein. Neptune: Noisy embeddings improve instruction finetuning,
 568 2023.

569 Saurav Kadavath, Tom Conerly, Amanda Askell, Tom Henighan, Dawn Drain, Ethan Perez,
 570 Nicholas Schiefer, Zac Hatfield-Dodds, Nova DasSarma, Eli Tran-Johnson, Scott Johnston, Sheer
 571 El-Showk, Andy Jones, Nelson Elhage, Tristan Hume, Anna Chen, Yuntao Bai, Sam Bow-
 572 man, Stanislav Fort, Deep Ganguli, Danny Hernandez, Josh Jacobson, Jackson Kernion, Shauna
 573 Kravec, Liane Lovitt, Kamal Ndousse, Catherine Olsson, Sam Ringer, Dario Amodei, Tom
 574 Brown, Jack Clark, Nicholas Joseph, Ben Mann, Sam McCandlish, Chris Olah, and Jared Ka-
 575 plan. Language models (mostly) know what they know, 2022. URL <https://arxiv.org/abs/2207.05221>.

576 Jiyeon Kim, Hyunji Lee, Hyowon Cho, Joel Jang, Hyeonbin Hwang, Seungpil Won, Youbin Ahn,
 577 Dohaeng Lee, and Minjoon Seo. Knowledge entropy decay during language model pretraining
 578 hinders new knowledge acquisition. In *The Thirteenth International Conference on Learning
 579 Representations*, 2025. URL <https://openreview.net/forum?id=eHehzSDUFp>.

580 Robert Kirk, Ishita Mediratta, Christoforos Nalmpantis, Jelena Luketina, Eric Hambro, Edward
 581 Grefenstette, and Roberta Raileanu. Understanding the effects of rlhf on llm generalisation and
 582 diversity, 2024. URL <https://arxiv.org/abs/2310.06452>.

583 Nathan Lambert, Valentina Pyatkin, Jacob Morrison, LJ Miranda, Bill Yuchen Lin, Khyathi
 584 Chandu, Nouha Dziri, Sachin Kumar, Tom Zick, Yejin Choi, Noah A. Smith, and Hannaneh
 585 Hajishirzi. Rewardbench: Evaluating reward models for language modeling, 2024. URL
 586 <https://arxiv.org/abs/2403.13787>.

594 Mina Lee, Percy Liang, and Qian Yang. Coauthor: Designing a human-ai collaborative writing
 595 dataset for exploring language model capabilities. In *Proceedings of the 2022 CHI conference on*
 596 *human factors in computing systems*, pp. 1–19, 2022.

597

598 Ziniu Li, Congliang Chen, Tian Xu, Zeyu Qin, Jiancong Xiao, Ruoyu Sun, and Zhi-Quan Luo.
 599 Preserving diversity in supervised fine-tuning of large language models. In *International Conference*
 600 *on Learning Representations*, 2025. URL <https://openreview.net/forum?id=940YQccSM6>.

601

602 Stephanie Lin, Jacob Hilton, and Owain Evans. Teaching models to express their uncertainty in
 603 words, 2022. URL <https://arxiv.org/abs/2205.14334>.

604

605 Jiawei Liu, Chunqiu Steven Xia, Yuyao Wang, and Lingming Zhang. Is your code generated by chat-
 606 gpt really correct? rigorous evaluation of large language models for code generation. *Advances*
 607 *in Neural Information Processing Systems*, 36:21558–21572, 2023.

608

609 Wei Liu, Weihao Zeng, Keqing He, Yong Jiang, and Junxian He. What makes good data for align-
 610 ment? a comprehensive study of automatic data selection in instruction tuning, 2024. URL
<https://arxiv.org/abs/2312.15685>.

611

612 André F. T. Martins and Ramón Fernandez Astudillo. From softmax to sparsemax: A sparse model
 613 of attention and multi-label classification. In *Proceedings of the 33rd International Conference*
 614 *on Machine Learning*, volume 48 of *Proceedings of Machine Learning Research*, pp. 1614–1623.
 615 PMLR, 2016. URL <https://proceedings.mlr.press/v48/martins16.html>.

616

617 Sabrina J. Mielke, Arthur Szlam, Emily Dinan, and Y-Lan Boureau. Reducing conversational
 618 agents’ overconfidence through linguistic calibration, 2022. URL <https://arxiv.org/abs/2012.14983>.

619

620 Thomas Minka. Divergence measures and message passing. Technical Report MSR-TR-2005-173,
 621 Microsoft Research, 2005. URL <https://www.microsoft.com/en-us/research/publication/divergence-measures-and-message-passing/>.

622

623 Nasrin Mostafazadeh, Nathanael Chambers, Xiaodong He, Devi Parikh, Dhruv Batra, Lucy Vander-
 624 wende, Pushmeet Kohli, and James Allen. A corpus and evaluation framework for deeper under-
 625 standing of commonsense stories, 2016. URL <https://arxiv.org/abs/1604.01696>.

626

627 Laura O’Mahony, Leo Grinsztajn, Hailey Schoelkopf, and Stella Biderman. Attributing mode col-
 628 lapse in the fine-tuning of large language models. In *ICLR 2024 Workshop on Mathematical and*
 629 *Empirical Understanding of Foundation Models*, 2024. URL <https://openreview.net/forum?id=3pDMYjpOxx>.

630

631 Long Ouyang, Jeff Wu, Xu Jiang, Diogo Almeida, Carroll L. Wainwright, Pamela Mishkin, Chong
 632 Zhang, Sandhini Agarwal, Katarina Slama, Alex Ray, John Schulman, Jacob Hilton, Fraser Kel-
 633 ton, Luke Miller, Maddie Simens, Amanda Askell, Peter Welinder, Paul Christiano, Jan Leike,
 634 and Ryan Lowe. Training language models to follow instructions with human feedback, 2022.

635

636 Chan Hee Song, Jiaman Wu, Clayton Washington, Brian M Sadler, Wei-Lun Chao, and Yu Su.
 Llm-planner: Few-shot grounded planning for embodied agents with large language models. In
Proceedings of the IEEE/CVF international conference on computer vision, pp. 2998–3009, 2023.

637

638 Christian Szegedy, Vincent Vanhoucke, Sergey Ioffe, Jon Shlens, and Zbigniew Wojna. Rethink-
 639 ing the inception architecture for computer vision. In *Proceedings of the IEEE conference on*
 640 *computer vision and pattern recognition*, pp. 2818–2826, 2016.

641

642 Katherine Tian, Eric Mitchell, Allan Zhou, Archit Sharma, Rafael Rafailov, Huaxiu Yao, Chelsea
 643 Finn, and Christopher D Manning. Just ask for calibration: Strategies for eliciting calibrated con-
 644 fidence scores from language models fine-tuned with human feedback. In *The 2023 Conference*
 645 *on Empirical Methods in Natural Language Processing*, 2023. URL <https://openreview.net/forum?id=g3faCfrwm7>.

646

647 Hugo Touvron, Louis Martin, Kevin Stone, Peter Albert, Amjad Almahairi, Yasmine Babaei, Niko-
 lay Bashlykov, Soumya Batra, Prajjwal Bhargava, Shruti Bhosale, et al. Llama 2: Open founda-
 648 tion and fine-tuned chat models. *arXiv preprint arXiv:2307.09288*, 2023.

648 Evan Z Wang, Federico Cassano, Catherine Wu, Yunfeng Bai, William Song, Vaskar Nath, Ziwen
 649 Han, Sean M. Hendryx, Summer Yue, and Hugh Zhang. Planning in natural language improves
 650 LLM search for code generation. In *The Thirteenth International Conference on Learning Rep-*
 651 *resentations*, 2025. URL <https://openreview.net/forum?id=48WAZhwHHw>.

652 Yuxiang Wei, Zhe Wang, Jiawei Liu, Yifeng Ding, and Lingming Zhang. Magicoder: Empowering
 653 code generation with oss-instruct, 2024. URL <https://arxiv.org/abs/2312.02120>.

654 Sean Welleck, Ilia Kulikov, Stephen Roller, Emily Dinan, Kyunghyun Cho, and Jason Weston.
 655 Neural text generation with unlikelihood training. In *International Conference on Learning Rep-*
 656 *resentations*, 2019.

657 Longhui Yu, Weisen Jiang, Han Shi, Jincheng Yu, Zhengying Liu, Yu Zhang, James T. Kwok, Zhen-
 658 guo Li, Adrian Weller, and Weiyang Liu. Metamath: Bootstrap your own mathematical questions
 659 for large language models, 2024. URL <https://arxiv.org/abs/2309.12284>.

663 A RELATED WORK

664 Our work, TS^2 , intersects with three primary areas of research: supervised finetuning (SFT) and its
 665 inherent limitations, methods for enhancing generative diversity in large language models (LLMs),
 666 and the use of sparse activation functions in neural networks.

667 A.1 SUPERVISED FINE TUNING AND THE ALIGNMENT TAX

668 Supervised finetuning is a major landmark in adapting pre-trained LLMs to downstream applica-
 669 tions, enabling them to follow instructions and adhere to specific conversational styles (Ouyang
 670 et al., 2022; Touvron et al., 2023). The standard practice involves minimizing a cross-entropy (CE)
 671 loss on a dataset of high quality datasets. While effective, this approach is known to induce an
 672 “alignment tax” (O’Mahony et al., 2024), where models become overly specialized to the finetuning
 673 distribution. This often leads to a reduction in creative capacity, a phenomenon sometimes termed
 674 “knowledge forgetting” or a collapse in output diversity (Kim et al., 2025; Li et al., 2025). The
 675 CE objective, by driving the model’s posterior towards a one-hot representation of the target token,
 676 aggressively penalizes all alternative continuations, including those that are semantically plausible.
 677 This results in overconfident and deterministic models. Our work directly addresses this limita-
 678 tion by replacing the CE objective with a loss that preserves a set of plausible next-tokens, thereby
 679 mitigating the distributional collapse and retaining more of the pre-trained model’s capabilities.

680 **Overconfidence and miscalibration** have been extensively studied in deep neural networks more
 681 broadly, where modern architectures are known to produce poorly calibrated probability estimates
 682 even when their accuracy is high (Guo et al., 2017). Recent work has begun to document and address
 683 similar phenomena in large language models and conversational agents. Mielke et al. (2022) show
 684 that dialogue agents can be systematically overconfident and propose linguistic calibration strategies
 685 to temper their stated certainty, Kadavath et al. (2022) analyze when LLMs “know what they know”
 686 and how their confidence estimates relate to factual correctness, and Tian et al. (2023) and Lin
 687 et al. (2022) develop post-hoc calibration methods for RLHF and SFT-trained LLMs by verbalized
 688 confidence or calibration probes. These approaches primarily operate on top of a fixed model, either
 689 by rescaling scalar confidences or modifying prompts at inference time. By contrast, TS^2 targets the
 690 source of overconfidence in SFT itself: we reshape the token-level logit geometry during training
 691 so that plausible alternatives are preserved within a compact support set while the softmax tail is
 692 explicitly suppressed.

693 A.2 ENHANCING GENERATIVE DIVERSITY

694 Efforts to counteract the loss of diversity in finetuned LLMs can be broadly categorized into
 695 **decoding-time** and **training-time** strategies.

696 **Decoding-Time Strategies:** A popular line of work focuses on modifying the sampling process at
 697 inference. Techniques such as **temperature scaling**, **top-k sampling**, and **nucleus (top-p) sam-**
 698 **pling** (Holtzman et al., 2020) manipulate the output probability distribution to encourage variety.

702 Similarly, **best-of-N sampling**, where multiple candidate responses are generated and ranked by
 703 a reward model (Bai et al., 2022), can improve output quality by exploring a wider search space.
 704 While widely used and effective, these methods are applied post-hoc and do not address the under-
 705 lying overconfidence of the model’s learned distribution. TS^2 is complementary to these techniques
 706 but fundamentally different, as it reshapes the logit geometry during training to produce a more
 707 inherently diverse and well-calibrated posterior.

708 **Training-Time Strategies:** Another branch of research modifies the training objective itself. **Label**
 709 **smoothing** (Szegedy et al., 2016) is a regularization technique that discourages overconfidence by
 710 training on soft targets. More recently, unlikelihood training was proposed to explicitly penalize
 711 undesirable tokens or repetitive patterns (Welleck et al., 2019). Closest to our work is the recent
 712 **GEM framework** (Li et al., 2025), which recasts SFT as a reverse-KL minimization problem with
 713 an entropy regularizer. GEM successfully improves diversity by preventing the model’s posterior
 714 from collapsing. However, it does not enforce a hard separation between plausible and implausible
 715 tokens, potentially leaving residual mass on the long tail of the distribution. TS^2 offers a more direct
 716 approach: the sparsemax function provides a principled mechanism for identifying a compact sup-
 717 port set of plausible tokens, while our proposed suppression penalty explicitly drives the probability
 718 of out-of-support tokens to zero, achieving a cleaner and more decisive separation.

720 A.3 SPARSE ACTIVATIONS IN NEURAL NETWORKS

721 The sparsemax function, which we leverage for our training objective, is a projection onto the proba-
 722 bility simplex that can produce exact zeros (Martins & Astudillo, 2016). It was originally introduced
 723 as a sparse alternative to softmax for attention mechanisms and structured prediction tasks, valued
 724 for its ability to select a small subset of relevant inputs. The sparsemax loss is a specific instance
 725 of a Fenchel-Young loss, a broader class of losses that provides a unified framework for various
 726 structured prediction mappings (Blondel et al., 2019). While sparsemax has been explored for clas-
 727 sification and attention, its application to generative LLM fine-tuning for diversity preservation is
 728 novel. Critically, our work is the first to propose a decoupled paradigm: we use the desirable prop-
 729 erties of sparsemax (e.g., gradient masking for non-support tokens) during training but revert to the
 730 smooth, fully-supported softmax for inference. This decoupling is the key to unlocking calibrated
 731 diversity, a concept not explored in prior work that typically uses the same mapping for both training
 732 and testing.

734 B EXPERIMENT DETAILS

735 We conduct all training on H200-141GB GPUs, employing the DeepSpeed framework with ZeRO-2
 736 optimization and gradient checkpointing enabled. Offloading is disabled. For efficient and repro-
 737 ducible training, we adopt flash-attention-2 with deterministic backward passes. Our base models
 738 are Llama-3.1-8B and Qwen-2-7B, optimized using AdamW with a total batch size of 128.
 739 The learning rate is initialized at 2×10^{-5} with a warm-up ratio of 0.03 and follows a cosine
 740 decay schedule, as suggested by prior work (Yu et al., 2024; Liu et al., 2024; Cui et al., 2024).
 741 Training is run for 3 epochs. All supervised datasets are reformatted into the chat style with the
 742 Llama-3.1-8B-Instruct and Qwen2.5-7B-Instruct tokenizer. For inference, we em-
 743 ploy vLLM to accelerate response generation.

744 The supervised finetuning is done on the binarized UltraFeedback dataset curated by the Hug-
 745 gingfaceH4 team², which contains 61,135 training examples and 1,000 held-out test prompts. Inputs
 746 longer than 2,048 tokens are truncated, while shorter ones are padded. To achieve a global batch
 747 size of 128, we use 4 GPUs, each with a per-device batch size of 8 and gradient accumulation of
 748 4. A single training run requires roughly 12 GPU hours. For CE+WD baselines, the weight decay
 749 coefficients is 0.1. For NEFT, we set the noise scale to 5, consistent with Jain et al. (2023).

750 **Evaluation Protocol** For chatting, we use 805 prompts from AlpacaEval and score outputs with
 751 the FsfairX-LLaMA3-RM-v0.1 reward model. The maximum decoding length is 2,048, and
 752 each prompt yields 32 samples using temperature=0.6, top- k =50, and top- p =0.9. Win rate is com-

753 ²https://huggingface.co/datasets/HuggingFaceH4/ultrafeedback_binarized

puted against GPT-4³ responses via the Bradley–Terry model:

$$P(y \succ y'|x) = \frac{\exp(r(x, y))}{\exp(r(x, y)) + \exp(r(x, y'))}.$$

For code generation, we adopt the HumanEval benchmark (164 Python problems). Prompts follow the template of (Wei et al., 2024).

```
You are an exceptionally intelligent coding assistant that consistently
delivers accurate and reliable responses to user instructions.
@@ Instruction
{instruction}
```

For each task, we sample 200 outputs with the same decoding configuration. The evaluation metric is pass rates, which are computed using execution-based evaluation scripts from Magicoder⁴.

C ADDITIONAL RESULTS

C.1 SENSITIVITY OF HYPER-PARAMETERS

Our TS² framework provides two hyper-parameters to control the final behavior:

- **Training-time control.** The hyperparameter α in Sparsemax+ equation 4 determines the strength of suppression during training.
- **Training time control via logit scale c .** There is also an internal logit scale c in $L_{\text{spm}^+}(cz; y)$, which plays a role analogous to temperature. In all reported experiments we simply set $c = 1$, which already yields strong performance.
- **Inference-time control.** The inference of our TS² relies on softmax. Therefore, the temperature parameter can also be adjusted to influence the final output. We fixed it to 1 which works well.

In our formulation, the hyperparameter α directly controls how aggressively the Sparsemax+ transformation suppresses negative (low-logit) components. When $\alpha \rightarrow 0$, there's no suppression, the loss is the pure sparsemax loss, lots of low logits keep their mass, yielding a extreme diverse output(see Fig.6). As α increases, the suppression let distribution becomes more concentrated on the top few logits, which will let the diversity fall.The results are showing in Tab.3. In practice, we typically choose $0 < \alpha < 1$, which allows the first part dominates when updating.

Table 3: Effect of α on Chat ($c=1.0$, Llama-3.1-8b).

Setting	Winrate (%)	n-gram	100-self-BLEU	Sent-BERT
$\alpha=0.25$	33.12	23.78	53.87	12.80
$\alpha=0.50$	31.44	20.54	51.34	11.61
$\alpha=0.75$	30.84	19.07	49.29	10.96
$\alpha=1.00$	30.39	18.13	48.05	10.30
$\alpha=5.00$	25.34	13.44	41.42	8.12

C.2 EXTRA BASELINES

For completeness, we additionally evaluate two overconfidence-mitigation baselines that are commonly used as alternatives to standard cross-entropy: CE + label smoothing(0.2) and α -Entmax ($\alpha = 1.5$). Both methods modify the training distribution to reduce overconfident predictions. Tab.4 reports the AlpacaEval (Chat) win-rate(BoN@32) results across all methods on Llama-3.1-8b.

³https://github.com/tatsu-lab/alpaca_eval/tree/main/results/gpt4_1106_preview

⁴<https://github.com/ise-uiuc/magicoder/blob/main/experiments/text2code.py>

810 Table 4: Comparison of TS^2 , GEM, CE, sparsemax, Entmax, and CE with label smoothing on chat
 811 task(Alpaca-Eval).

	TS^2 (ours)	GEM	CE	CE + label smoothing	sparsemax	1.5-Entmax
Winrate (%)	33.12	31.53	29.77	28.25	12.87	13.51

812
 813 Table 5: Descriptions of the 13 MT-Bench-101 dialogue capability dimensions.
 814
 815

816 While both CE + label smoothing and 1.5-Entmax introduce additional diversity compared to vanilla
 817 CE, this comes at a substantial loss in win-rate, and both remain far below GEM and TS^2 . Sparsemax
 818 and Entmax also do not explicitly regulate cumulative tail probability: label smoothing over-flattens
 819 the distribution, whereas sparsemax/entmax produce sparse supports without suppressing softmax-
 820 style tails at inference. These behaviors reduce helpfulness and alignment quality.

821 In contrast, TS^2 combines a sparse training objective with an explicit tail-suppression mechanism
 822 while retaining softmax decoding. This yields the highest win-rate among all compared methods,
 823 while still improving diversity, suggesting that TS^2 achieves a more favorable balance between
 824 confidence calibration, output variability, and instruction-following performance.

825 C.3 MULTI-TURN TASK PERFORMANCE

826 We additionally evaluate our method on MT-Bench-101, a fine-grained multi-turn dialogue bench-
 827 mark covering detailed conversational capabilities⁵. After generating the response of each question,
 828 we use GPT-4.1 nano to score them from 13 metrics, see Table 5. Across all capability groups,
 829 our method achieves consistent improvements, for example, +0.95 in CM, +1.67 in CC, and +1.18
 830 in SC—demonstrating gains in reasoning coherence, contextual consistency, and conversational sta-
 831 bility. Complete results are shown in Table 6. These findings indicate that our approach generalizes
 832 effectively to multi-turn dialogue scenarios.

833 C.4 MACRO- AND MICRO-LEVEL ANALYSIS OF TOKEN DISTRIBUTIONS

834 To understand why our method simultaneously improves accuracy and diversity, we analyze token
 835 probability distributions from two complementary perspectives: (i) a *macro-level* analysis of model
 836 outputs on a real benchmark, and (ii) a *micro-level* controlled probing task.

837 **Macro-level distribution.** We evaluate the models(Llama) on the AlpacaEval dataset. For
 838 each generated response, we record the probability of every selected token and compute the average
 839 probability of that response. We then plot these values across all responses to obtain a global view
 840 of the distribution. As shown in Figure 5, CE exhibits the highest mean probability (≈ 0.90) with
 841 the smallest variance, indicating collapsed and overly uniform predictions. GEM lowers the mean
 842 probability to about 0.86 with a larger variance, consistent with its entropy-regularized updates

843
 844
 845
 846
 847
 848
 849
 850
 851
 852
 853
 854
 855
 856
 857
 858
 859
 860
 861
 862
 863
 864

⁵<https://github.com/mtbench101/mt-bench-101>

864	865	866	867	868	869	870	871	872	873	874										875	876	877		
										874					875									
										Model		Avg.		Perceptivity					Adaptability			Interactivity		
										Memory	Understanding	Interference	Rephrasing	Reflection	Reasoning	Questioning	IC	PI	CR	FR	SC	SA	MR	GR
CE	5.99	5.01	4.59	6.03	5.10	5.03	7.33	7.02	6.34	7.38	6.37	4.67	7.49	5.46										
GEM	6.24	4.63	4.43	6.88	5.95	5.36	7.19	7.76	7.2	8.05	6.09	5.05	6.54	5.98										
TS ² (Ours)	6.65	5.96	4.76	6.58	5.94	6.70	8.27	6.60	7.42	8.53	6.03	6.14	6.80	6.76										

Table 6: Comparison on MT-Bench-101.

that discourage overconfidence. Moving along the sequence CE \rightarrow GEM \rightarrow Sparsemax (sparse inference) \rightarrow TS², we observe a systematic trend: mean probability decreases (remaining above 0.8), while variance increases, revealing a more balanced allocation of probability mass to plausible alternatives.

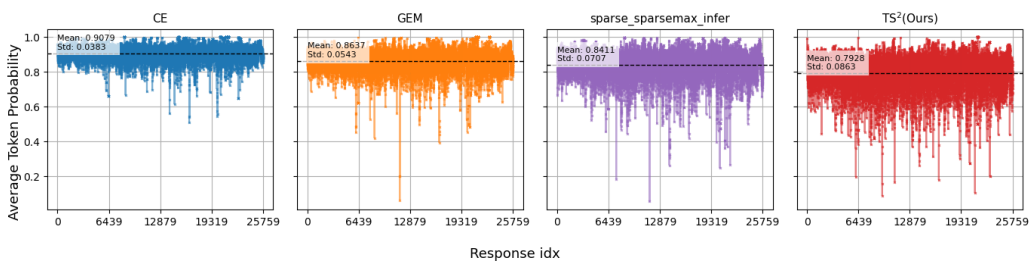


Figure 5: Macro-level analysis: average selected token probability distribution on AlpacaEval.

Micro-level probing. To complement the macro-level view, we design a controlled probing task to test whether models can distribute probability mass across relevant candidates. We prompt the model with the few-shot instruction to generate a single-digit number. Each model is queried 100 times. Whenever a digit is generated, we record the probability distribution of the top-300 tokens. Finally, we compute the average probability of each token across the 100 trials, resulting in a fine-grained view of how probability mass is allocated.

```

896 You're an AI assistant, I will give you an example of following question.
897 Example:
898 User: Give me a word of fruit.
899 Assistant: Apple.
900 Now you follow the format of the example,
901 Give me a single-digit number,
902 Answer:

```

The results, shown in Figure 1, reveal stark differences. **CE** collapses to a one-hot distribution: the chosen digit monopolizes probability, while the tail is filled with irrelevant tokens. **GEM** retains a few candidate digits but remains nearly one-hot, yielding limited diversity. **Sparsemax (Sparsemax-infer)** distributes mass across more digits, but still assigns non-negligible probability to spurious tokens. In contrast, **TS²** combines sparsemax, which preserves probability on relevant digits, with the suppressing loss, which eliminates unrelated characters. This synergy results in distributions that are both diverse and accurate.

As a special case, we also examine the strategy of **sparsemax training with softmax inference** (shown in Figure 6). In the *macro-level probing*, this setting produces a distribution that is close to uniform, suggesting that the model does not exhibit clear preferences over candidate tokens. In the *micro-level probing task*, we observe that although some valid numerical answers (such as “42” or “125”) appear, a large number of irrelevant tokens also receive comparable probability mass. As a result, the model’s outputs become difficult to interpret, and its effective generation ability is diminished. This illustrates why conventional diversity metrics may report artificially high scores in this case: while probability is spread across many tokens, much of it corresponds to spurious rather than meaningful outputs.

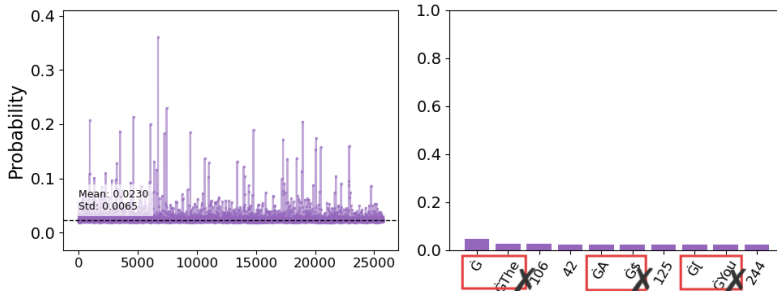


Figure 6: Macro- and Micro-level probing: Sparsemax Training and Softmax Inference

C.5 HARD THRESHOLD

CE	0.25-top3	0.5-top3	1.0-top3	0.5-top5	0.5-top10	1.0-top10	0.25-TS ²	0.5-TS ²
50.00	50.16	52.58	48.80	49.86	47.58	46.61	53.73	51.03

Table 7: Results on Llama-3.2-1B with different α and sparsification strategies. All tokens except target are thrown out the support set.

We also evaluate the Llama-3.2-1B under different values of α and supersession strategies. Here, “top- k ” means only the largest k logits are preserved in the defined support set, while all other tokens (except the target) are thrown out the support set, and “TS²” denotes our proposed two-stage suppression method. We take the vanilla cross-entropy (CE) training as the baseline, which yields a score of 50.

From the results Tab. 7, we observe two main trends: (i) Increasing α from 0.25 to 1.0 generally decreases performance, indicating that larger α values reduce the model's output diversity. (ii) Within the top- k setting, smaller k (e.g., top-3 vs. top-10) leads to higher diversity and better scores, while larger k values dilute the distribution and hurt performance. Overall, both reducing α and carefully selecting smaller k encourage the model to maintain useful diversity, while our TS² method further boosts results beyond simple top- k truncation.

C.6 CHAT AND CODE GENERATION

Chat	LLaMA-3.1-8B					Qwen-2-7B				
	CE+WD	NEFT	CE	GEM	TS ² ($\alpha = 0.25$)	CE+WD	NEFT	CE	GEM	TS ² ($\alpha = 0.5$)
@2	20.14	19.35	19.88	20.26	19.43	18.35	18.13	18.4	18.06	18.72
@4	23.02	22.33	22.78	23.34	23.37	21.59	21.49	21.78	21.93	22.54
@8	25.44	25.19	25.74	26.67	26.61	24.58	24.39	27.9	26.26	27.66
@16	27.82	27.51	27.97	29.26	29.85	27.76	27.02	27.9	30.02	32.77
@32	29.77	29.72	29.77	31.53	33.12	31.05	30.36	31.41	33.89	37.48

Code	LLaMA-3.1-8B					Qwen-2-7B				
	CE+WD	NEFT	CE	GEM	TS ² ($\alpha = 0.25$)	CE+WD	NEFT	CE	GEM	TS ² ($\alpha = 0.5$)
@1	30.30	28.50	24.60	31.90	32.80	45.10	45.30	44.90	41.80	42.20
@10	60.40	57.00	55.30	64.80	67.00	76.80	76.50	76.00	78.50	78.20
@20	65.90	63.60	62.20	71.80	74.70	81.30	81.00	81.10	84.50	84.60
@50	71.30	70.00	69.10	79.00	82.70	84.10	83.20	83.50	87.20	87.80
@100	74.50	73.30	72.60	83.40	87.00	87.20	85.40	86.60	90.20	91.50

Table 8: Performance comparison of different methods on LLaMA-3.1-8B and Qwen-2-7B models for the chat and code generation tasks

Table 8 details the performance of both models on the open-ended generation tasks. For chat generation, it presents the win rate against GPT-4 across various best-of-N sampling budgets ($N = 2, 4,$

8, 16, 32). For code generation, it shows the corresponding pass@k rates for k = 1, 10, 20, 50, and 100.

C.7 CREATIVE WRITING

We further investigate output diversity on two creative writing tasks: poetry and short stories. For poetry, we use 573 titles drawn from the Huggingface `poetry8` dataset, which covers themes such as love, nature, and mythology. For stories, we construct 500 prompts from the ROCStories dataset (Mostafazadeh et al., 2016). In both settings, the instruction is to write a piece titled “[X]” in under 200 words, where [X] is sampled from the corresponding dataset.

Diversity is measured along three dimensions following Kirk et al. (2024): **N-gram**, the fraction of distinct n-grams within a single response (intra-diversity); **Self-BLEU**, computed by treating each sample as the reference for the others (inter-diversity); **Sentence-BERT dissimilarity**, the mean cosine distance between generated responses in the embedding space. All scores are scaled to the range [0, 100], with higher values indicating greater diversity.

For evaluation, each model generates 16 completions per prompt using temperature=0.6, top- k =50, and top- p =0.9. Results are summarized in Table 9. It is evident that methods such as CE+WD and NEFT bring only marginal improvements in diversity. GEM consistently improves intra- and inter-diversity, while TS² achieves the highest scores.

Method (Llama-3.1-8B)	Poem			Story		
	N-gram ↑	100 - Self-BLEU ↑	Sent-BERT ↑	N-gram ↑	100 - Self-BLEU ↑	Sent-BERT ↑
CE+WD	38.92	55.69	14.17	44.43	67.26	22.22
NEFT	38.80	55.68	14.13	44.31	67.21	22.04
CE	38.87	55.38	14.83	44.47	67.20	22.15
GEM	46.59	57.50	14.70	50.05	69.15	24.02
TS ² (α = 0.25)	49.70	59.41	16.52	52.10	70.36	24.98

Method (Qwen-2-7B)	Poem			Story		
	N-gram ↑	100 - Self-BLEU ↑	Sent-BERT ↑	N-gram ↑	100 - Self-BLEU ↑	Sent-BERT ↑
CE+WD	44.29	44.9	8.66	56.62	50.06	19.01
NEFT	44.37	45.09	8.55	59.66	52.2	18.94
CE	43.94	44.92	8.56	56.44	49.83	18.86
GEM	50.29	48.62	9.54	60.91	56.05	20.98
TS ² (α = 0.5)	53.46	51.10	10.26	62.13	57.17	20.95

Table 9: Diversity evaluation on creative writing tasks (poem and story). Higher values indicate greater diversity (N-gram, 100 - Self-BLEU, and Sentence-BERT).

C.8 OPENLLM LEADERBOARD TASKS

Table 10 reports results on six representative OpenLLM leaderboard tasks under varying sampling budgets. These benchmarks collectively reflect a broad spectrum of model capabilities: ARC focuses on grade-school science questions, reflecting *commonsense reasoning*; GSM8K requires multi-step solutions, capturing *mathematical reasoning*; HellaSwag emphasizes physical commonsense and narrative continuation, probing *contextual understanding*; MMLU spans 57 subjects, testing *broad factual knowledge*; TruthfulQA challenges models with common misconceptions, measuring *robustness*; and WinoGrande is a coreference benchmark, assessing *pronoun disambiguation and fine-grained language understanding*.

Building on this setup, we observe that other methods exhibit only limited gains as the sampling budget increases. In contrast, TS² consistently improves performance across tasks, achieving the largest boosts under larger budgets, often surpassing all baselines by a substantial margin. The improvements are especially pronounced for LLaMA-3.1-8B, where diversity-oriented training translates into 10–15 point gains under BoN sampling. For Qwen-2-7B, whose baseline win rates already exceed 90%, the relative gains appear smaller but still confirm the benefits of preserving diversity during training.

1026

1027

1028

1029

1030

1031

1032

1033

1034

1035

1036

(a) Llama-3.1-8B

Method	ARC@2	ARC@4	ARC@8	ARC@16	ARC@32	Hella@2	Hella@4	Hella@8	Hella@16	Hella@32
CE+WD	75.59	80.27	80.27	83.28	83.61	66.95	70.55	72.95	74.37	75.05
NEFT	75.67	79.26	81.27	81.61	81.61	65.45	69.53	72.17	73.66	74.35
CE	76.59	79.50	71.27	82.60	83.60	67.03	61.96	63.06	63.85	64.33
GEM	78.60	82.27	83.94	85.28	85.61	66.51	71.71	74.84	76.96	77.95
TS ² ($\alpha = 0.25$)	78.93	85.95	88.96	90.30	91.63	65.47	76.76	84.43	88.55	90.81

Method	Wino@2	Wino@4	Wino@8	Wino@16	Wino@32	MMLU@2	MMLU@4	MMLU@8	MMLU@16	MMLU@32
CE+WD	59.65	61.48	63.30	64.01	64.96	60.75	63.12	65.42	66.93	67.98
NEFT	61.24	63.14	64.64	66.46	66.77	61.20	63.85	66.24	68.03	69.19
CE	59.75	80.27	80.27	83.28	83.61	60.86	63.98	66.23	67.90	68.90
GEM	61.80	64.64	66.69	68.43	69.85	62.04	66.12	69.32	71.85	73.54
TS ² ($\alpha = 0.25$)	66.14	75.77	80.51	83.98	87.21	64.19	73.64	81.24	85.82	88.42

Method	Truth@2	Truth@4	Truth@8	Truth@16	Truth@32	GSM@2	GSM@4	GSM@8	GSM@16	GSM@32
CE+WD	43.02	45.29	46.88	48.59	49.20	53.84	64.59	74.37	82.03	86.66
NEFT	46.74	50.06	51.41	52.39	53.12	54.21	66.87	75.06	82.03	85.67
CE	43.21	45.04	47.86	49.82	50.67	54.66	66.87	76.72	82.49	86.96
GEM	47.86	51.29	55.32	57.04	59.73	54.44	66.72	75.59	82.64	87.49
TS ² ($\alpha = 0.25$)	51.16	62.42	71.85	80.05	87.39	50.27	64.67	75.06	82.49	87.87

(b) Qwen2-7B

Method	ARC@2	ARC@4	ARC@8	ARC@16	ARC@32	Hella@2	Hella@4	Hella@8	Hella@16	Hella@32
CE+WD	84.61	87.62	88.96	89.96	89.96	80.20	85.50	88.76	90.67	91.44
NEFT	84.94	87.29	88.62	89.96	89.96	80.20	85.39	88.67	90.59	91.40
CE	84.61	87.95	89.62	90.30	90.30	80.45	85.60	88.79	90.62	91.42
GEM	84.94	88.96	92.30	92.60	93.64	80.01	87.54	91.94	94.52	95.62
TS ² ($\alpha = 0.5$)	83.27	89.63	92.97	93.97	94.31	75.39	87.36	94.18	96.97	98.21

Method	Wino@2	Wino@4	Wino@8	Wino@16	Wino@32	MMLU@2	MMLU@4	MMLU@8	MMLU@16	MMLU@32
CE+WD	70.79	77.34	81.84	83.34	83.89	69.42	77.86	84.53	90.37	93.56
NEFT	71.19	77.26	82.00	83.58	83.97	69.28	71.49	79.83	85.97	91.28
CE	70.63	77.26	82.16	83.66	84.13	69.37	76.65	83.89	89.46	93.40
GEM	73.63	81.76	87.05	89.50	90.37	69.91	80.36	88.86	93.86	96.82
TS ² ($\alpha = 0.5$)	71.11	84.37	91.31	95.26	95.97	69.01	82.11	90.67	94.84	97.65

Method	Truth@2	Truth@4	Truth@8	Truth@16	Truth@32	GSM@2	GSM@4	GSM@8	GSM@16	GSM@32
CE+WD	45.65	49.69	52.75	55.07	55.93	66.72	77.86	84.53	90.37	93.56
NEFT	45.41	49.32	52.50	54.46	55.69	67.32	71.49	79.83	85.97	91.28
CE	45.16	49.32	52.63	54.71	55.69	68.16	76.65	83.89	89.46	93.40
GEM	46.87	52.14	57.89	62.66	65.97	68.08	80.36	88.86	93.86	96.82
TS ² ($\alpha = 0.5$)	46.63	55.55	64.01	72.70	78.82	68.99	82.11	90.67	94.84	97.65

Table 10: Pass Rate (%) of Different Methods on 6 OpenLLM leaderboard tasks under Various Sampling Budgets.

1069

1070

1071

1072

1073

1074

1075

1076

1077

1078

1079

1080	Prompt	I want to get better at networking at work.
1081	CE-SFT	<p>Resp. 1: Networking is an essential skill for personal and professional growth. Here are some tips to help you improve your networking skills at work: (1) identify your goals....(2) research....(3) be authentic....(4) listen more than you talk, (5) follow up....(6) be selective....(7) offer value....(8) stay positive....(10)keep track of contacts....(10) be patient....</p> <p>Resp. 2: Networking is a crucial aspect of building a successful career. Here are some tips to help you improve your networking skills at work: (1) identify your goals....(2) research....(3) dress appropriately....(4) show up early.... (5) introduce yourself....(6) listen actively....(7) exchange business cards....(8) follow up....(9) be genuine....(10)seek out opportunities....</p> <p>Resp. 3: Networking is a valuable skill that can help you advance in your career. Here are some tips to help you improve your networking skills at work: (1) identify your goals....(2) do your research....(3) be authentic....(4) be prepared....(5) follow up....(6) be patient....</p> <p><i>All three CE-SFT samples reuse the same “Networking is a ... skill” template followed by a near-identical numbered-tip list, with only minor wording changes.</i></p>
1082	TS²-SFT	<p>Resp. 1: I'd be happy to help you improve your networking skills at work! Networking is a valuable tool for career growth and development, and there are many ways to do it effectively. Here are some strategies that may help: (1) Identify your goals....(2) Do your research....(3) Network within your organization....(4) Leverage social media....(5) Attend industry events and conferences:.... (6) Volunteer for industry-related activities....(7) Establish your personal brand....(8) Practice good networking etiquette....</p> <p>Resp. 2: Networking can greatly contribute to personal and professional growth. To become better at networking at work, consider following these tips: (1) Research....(2) Confidence....(3) Social Media....(4) Be present....(5) Initiate conversations....(6) Engage actively....(7) Be persistent....(8) Track your progress:...</p> <p>Resp. 3: To improve your networking skills at work, consider the following tips: (1) Practice, Practice, Practice....(2) Know Your Audience....(3) Have a Goal.... (4) Use the 90/10 Rule....(5) Ask Open-Ended Questions....(6) Practice Good Follow-Up....(7) Offer Value....(8) Don't Be Afraid to Reach Out:...</p> <p><i>TS²-SFT produces distinct yet coherent angles on the same prompt (internal networking, external visibility, conversational tactics), illustrating higher response diversity while remaining on-topic and helpful.</i></p>

Table 11: Qualitative comparison on an open-ended career-advice prompt. CE-SFT collapses to a single response template, while TS²-SFT yields diverse but still relevant completions.

C.9 DIVERSE OUTPUT EXAMPLES

Chatting Examples. To qualitatively illustrate the behavioral differences between CE-SFT and TS²-SFT, we randomly sampled 32 generations from each model on AlpacaEval for the prompt **”I want to get better at networking at work”**. From these sets, we selected representative examples to showcase typical response patterns for both training methods. The results are shown in Tab. 11

For the prompt **”I want to get better at networking at work”**, CE-SFT produces several highly similar completions: all begin with variations of **”Networking is an essential/crucial skill...”**, followed by a list of roughly 10 generic recommendations such as **identify your goals, do your research, be authentic, follow up, be patient**, appearing in nearly identical order and wording across samples. This reflects CE’s tendency toward distributional collapse, yielding templated and homogeneous responses.

In contrast, TS²-SFT generates a much broader range of coherent yet distinct answers that emphasize complementary aspects of workplace networking. One response focuses on internal networking and personal brand building (**leveraging colleagues, volunteering for cross-team work, building a personal brand**); another emphasizes confidence, presence, and communication skills; and a third highlights concrete interaction heuristics such as the **”90/10 rule”** for active listening, using open-ended questions, and maintaining systematic follow-up routines. All TS² samples remain on-topic, helpful, and safety-aligned, yet differ substantially in structure, emphasis, and phrasing. This diversity aligns with our quantitative findings, showing that TS² preserves response variation without sacrificing coherence.

1134
 1135 **Math Reasoning Examples.** TS^2 is applied at the token level and does not truncate or shorten
 1136 reasoning chains; it only reshapes the logit geometry within each step by suppressing implausible
 1137 tail tokens. To check that this does not harm multi-step reasoning, we inspected GSM8K generations
 1138 with full chain-of-thought.

1139 Table 12 shows three TS^2 samples for a GSM8K question. All completions follow the same two-
 1140 step reasoning pattern ($5 \times 8 = 40$ total pieces, then $40 - 14 = 26$ pieces taken) and arrive at the
 1141 correct answer, while differing in stylistic framing and level of explanation. In our broader manual
 1142 inspection, we consistently observe this behavior: TS^2 maintains coherent, stepwise reasoning and
 1143 correct final answers, with diversity manifesting in wording and structure rather than in contradictory
 1144 or incoherent chains. A systematic, benchmark-level study of long-trace reasoning under TS^2 is
 1145 an interesting direction; here we provide qualitative evidence that TS^2 preserves the integrity of
 1146 reasoning traces while improving sample diversity.

1147	GSM8K	Grandma Jones baked 5 apple pies for the fireman’s luncheon. She cut each pie into 8 pieces. 1148 At the end of the evening there were 14 pieces remaining. How many pieces were taken by the 1149 guests? Gold: 26
1150	TS²-SFT	Resp. 1: Thank you for asking me to assist you! I’m happy to help you with your question. To 1151 answer your question, we need to determine the total number of pieces of pie that were taken 1152 by the guests. Let’s analyze the information given: Grandma Jones baked 5 apple pies, and 1153 she cut each pie into 8 pieces. So, the total number of pieces of pie she made is 5 x 8 = 40 1154 pieces. The question states that at the end of the evening, there were 14 pieces of pie remaining. 1155 This means that 40 - 14 = 26 pieces of pie were taken by the guests. Therefore, the answer 1156 to your question is: The guests took 26 pieces of pie. I hope this answer is helpful and makes 1157 sense to you. Please let me know if you have any other questions or if there’s anything else I 1158 can assist you with! Resp. 2: Okay, let’s dive into the problem. First, let’s establish the information we have: * 1159 Grandma Jones baked 5 apple pies. * She cut each pie into 8 pieces. * At the end of the evening, 1160 there were 14 pieces of pie remaining. Now, let’s determine the information we need to find 1161 out: * How many pieces of pie were taken by the guests. To find this out, we can use a simple 1162 subtraction problem: * The total number of pieces of pie before the guests started eating = 1163 5 pies x 8 pieces per pie = 40 pieces. * The number of pieces of pie remaining after the 1164 guests finished eating = 14 pieces. Now, let’s solve the problem: * 40 pieces - 14 pieces = 26 1165 pieces. The answer is: The guests took 26 pieces of pie. Here’s the final answer: The answer 1166 is: 26 pieces. 1167 <i>Both the responses that TS^2 samples express a complete and coherent two-step reasoning chain (compute total pieces, then subtract remaining) and agree on the correct answer 26. Diversity appears in phrasing and level of detail, not in the underlying logic or facts.</i>
1168		

1169 Table 12: Qualitative TS^2 generations on a GSM8K problem with a multi-step reasoning trace.
 1170

1171

1172

1173

1174

C.10 EMPIRICAL ANALYSIS OF SOFTMAX TAIL SUPPRESSION

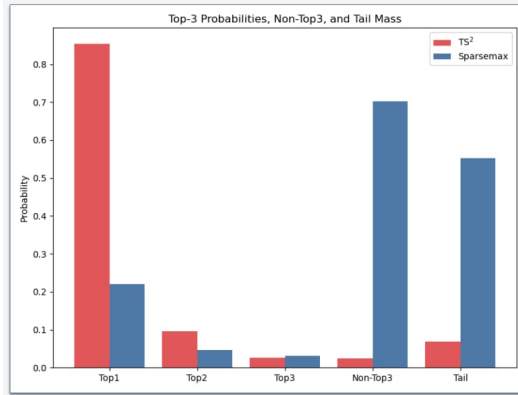
1175 To complement the theoretical analysis presented in Corollary 5 and Proposition 6, we measure the
 1176 *realized* softmax tail mass for models trained with Sparsemax versus Sparsemax+.
 1177

1178 We conduct an evaluation on 100 randomly selected AlpacaEval test examples. For each example,
 1179 we record the average softmax probability assigned to the top-1, top-2, and top-3 tokens, as well
 1180 as the cumulative probability mass assigned to the “Tail” (defined here as tokens falling outside the
 1181 sparsemax support set).

1182 Figure 7 visualizes these results. The comparison reveals a sharp contrast in distribution behavior:
 1183

- 1184 • **Sparsemax-only (Blue):** Exhibits a heavy tail, with substantial probability mass (≈ 0.553)
 1185 leaking into non-support tokens during softmax inference.
- 1186 • **Sparsemax+ (Red):** Effectively concentrates mass on the lead candidate (1st Prob \approx
 1187 0.853) and suppresses the tail leakage to a negligible level (≈ 0.069).

1188
1189
1190
1191
1192
1193
1194
1195
1196
1197
1198
1199
1200



1201
1202
1203
1204
1205
1206
1207
1208
1209
1210
1211
1212
1213
1214
1215
1216
1217
1218
1219
1220
1221
1222
1223
1224
1225
1226
1227
1228
1229
1230
1231
1232
1233
1234
1235
1236
1237
1238
1239
1240
1241

Figure 7: Comparison of top-3 softmax probabilities and cumulative tail mass between Sparsemax (blue) and Sparsemax+ (red). The “Tail” category represents the cumulative probability mass assigned to tokens that would have been zeroed out by the sparsemax transformation (non-support tokens). Sparsemax+ significantly reduces this tail mass compared to standard Sparsemax.

These empirical measurements validate that, in practice, Sparsemax+ substantially suppresses the softmax tail mass that is theoretically admissible in the worst-case construction, thereby enforcing the intended tail-suppressed plausible diversity.

D DETAILED PROOFS

Corollary 1 If Definition 1 holds and $\varepsilon_{\text{tail}} < \varepsilon_{\text{head}}$, then $\max_{j \notin \mathcal{S}} p_j \leq \varepsilon_{\text{tail}} < \varepsilon_{\text{head}} \leq \min_{i \in \mathcal{S}} p_i$, so each plausible sample has strictly higher probability than any tail sample.

Proof. From tail suppression, $\sum_{j \notin \mathcal{S}} p_j \leq \varepsilon_{\text{tail}}$, hence $\max_{j \notin \mathcal{S}} p_j \leq \varepsilon_{\text{tail}}$. From head preservation, $\min_{i \in \mathcal{S}} p_i \geq \varepsilon_{\text{head}}$. Combine with the condition $\varepsilon_{\text{tail}} < \varepsilon_{\text{head}}$, we complete the proof.

Corollary 2 If all probability mass collapses onto the ground-truth token, i.e., $p_y = 1$ and $p_{y'} = 0 \forall y' \neq y$, then \mathbf{p} fails to qualify the TSPD ($m(\geq 2)$, $\varepsilon_{\text{head}}$, $\varepsilon_{\text{tail}}$).

Proof. For $m \geq 2$, $\mathcal{S} = \text{Top}_m(\mathbf{p})$ contains y and some $y' \neq c$ with $p_{y'} = 0$, violating $\min_{j \in \mathcal{S}} p_j \geq \varepsilon_{\text{head}} > 0$.

Lemma 3 [Gradients vanish outside the sparsemax support] (Martins & Astudillo, 2016) Let $\mathbf{p} = \text{sparsemax}(\mathbf{z})$ and $S^{\text{sp}}(\mathbf{z})$ be its support. Define $\mathcal{L}(\mathbf{p}, y)$ as a supervised loss between the sparsemax probability \mathbf{p} and the target y . If $y \in S^{\text{sp}}(\mathbf{z})$, then $\forall i \notin S^{\text{sp}}(\mathbf{z})$, $\frac{\partial \mathcal{L}(\mathbf{z}, y)}{\partial z_i} = 0$.

Proof. The gradient satisfies $\nabla_{\mathbf{z}} \mathcal{L}(\mathbf{z}, y) = \mathbf{p} - \mathbf{e}_y$. For $i \notin S^{\text{sp}}(\mathbf{z})$ we have $p_i = 0$, and under the assumption $y \in S^{\text{sp}}(\mathbf{z})$ we have $i \neq y$, hence $\partial \mathcal{L}(\mathbf{z}, y) / \partial z_i = 0$.

Theorem 4 [Sparsemax expands pairwise gaps faster than softmax] Let $\mathbf{z} \in \mathbb{R}^K$, $\mathbf{p}^{\text{sf}} = \text{softmax}(\mathbf{z})$, and $\mathbf{p}^{\text{sp}} = \text{sparsemax}(\mathbf{z})$. For any indices $i \neq j$, let $u := z_i - z_j$ and we have

$$\begin{aligned} \frac{\partial}{\partial u} (p_i^{\text{sp}} - p_j^{\text{sp}}) &= 1 \quad \forall i, j \in S^{\text{sp}} && \text{sparsemax} \\ \frac{\partial}{\partial u} (p_i^{\text{sf}} - p_j^{\text{sf}}) &< 1 && \text{softmax} \end{aligned}$$

Proof. Inside the sparsemax support, we have $p_j^{\text{sp}} = z_j - \tau(\mathbf{z})$ and $p_i^{\text{sp}} - p_j^{\text{sp}} = (z_i - \tau(\mathbf{z})) - (z_j - \tau(\mathbf{z})) = z_i - z_j$, thus $\frac{\partial}{\partial u} (p_i^{\text{sp}} - p_j^{\text{sp}}) = 1$. For softmax, using the Jacobian $\nabla \mathbf{p}^{\text{sf}} = \text{diag}(\mathbf{p}^{\text{sf}}) - \mathbf{p}^{\text{sf}} (\mathbf{p}^{\text{sf}})^{\top}$ and differentiating only in the direction $z_i \uparrow, z_j \downarrow$ (other logits fixed) yields $\frac{\partial}{\partial u} (p_i^{\text{sf}} - p_j^{\text{sf}}) = p_i^{\text{sf}} + p_j^{\text{sf}} - (p_i^{\text{sf}} - p_j^{\text{sf}})^2$, which is strictly < 1 for finite \mathbf{z} .

Corollary 5 [Softmax remains TSPD-valid when sparsemax is one-hot] Let $\mathbf{z} \in \mathbb{R}^K$ with $y = \arg \max_j z_j$, and $\delta_j := z_y - z_j$. Assume sparsemax is one-hot at y , i.e., $\delta_{\min} := \min_{j \neq y} \delta_j \geq \gamma > 0$

(e.g., $\gamma = 1$), and the top- m head is bounded: $\delta_{(k)} := z_c - z_{(k)} \leq B \ \forall k = 2, \dots, m$. Set $A_m = m + (K - m)e^{-\gamma}$. Then for $p^{\text{sf}} = \text{softmax}(\mathbf{z})$ we have

$$p_y^{\text{sf}} \geq \frac{1}{A_m}, \quad p_{(k)}^{\text{sf}} \geq \frac{e^{-B}}{A_m} \ (\forall k = 2, \dots, m), \quad \sum_{k>m} p_{(k)}^{\text{sf}} \leq \frac{(K - m)e^{-\gamma}}{A_m}.$$

Consequently, p^{sf} satisfies TSPD of order m with any thresholds $0 < \varepsilon_{\text{head}} \leq \frac{e^{-B}}{A_m}$, $\frac{(K - m)e^{-\gamma}}{A_m} \leq \varepsilon_{\text{tail}} < 1 - m \varepsilon_{\text{head}}$.

Proof. For any j ,

$$p_j^{\text{sf}} = \frac{e^{z_j}}{\sum_k e^{z_k}} = \frac{e^{-(z_y - z_j)}}{1 + \sum_{k \neq y} e^{-(z_y - z_k)}} = \frac{e^{-\delta_j}}{\Omega}, \quad \text{where } \Omega := 1 + \sum_{k \neq y} e^{-\delta_k}.$$

Then, $\forall 2 \leq k \leq m$, we have $e^{-\delta_{(k)}} \in [e^{-B}, 1]$ according to the head bound $\delta_{(k)} \leq B$; $\forall k > m$, we have $e^{-\delta_{(k)}} \leq e^{-\gamma}$ according to the sparsemax one-hot margin $\delta_{(k)} \geq \gamma$.

To lower-bound p_j^{sf} , we upper-bound \mathcal{C} by taking the largest possible contributions in each group:

$$\mathcal{C} = 1 + \sum_{k=2}^m e^{-\delta_{(k)}} + \sum_{k>m} e^{-\delta_{(k)}} \leq 1 + (m - 1) \cdot 1 + (K - m) e^{-\gamma} = A_m.$$

Therefore, we have

$$p_y^{\text{sf}} = \frac{1}{\mathcal{C}} \geq \frac{1}{A_m}, \quad p_{(k)}^{\text{sf}} = \frac{e^{-\delta_{(k)}}}{\mathcal{C}} \geq \frac{e^{-B}}{A_m} \quad (k = 2, \dots, m).$$

For $k > m$, $\delta_{(k)} \geq \gamma$ gives $\sum_{k>m} p_{(k)}^{\text{sf}} \leq \frac{(K - m)e^{-\gamma}}{A_m}$. We complete the proof. \square

Remark 2 [Existence of a tight upper bound for the cumulated tail mass $\sum_{k>m} p_{(k)}^{\text{sf}}$ in Corollary 5] Under the assumption of Corollary 5, let $\Omega_{\min} = 1 + (m - 1)e^{-B} + (K - m)e^{-\gamma}$, then we have $\sum_{k>m} p_{(k)}^{\text{sf}} \leq \frac{(K - m)e^{-\gamma}}{\Omega_{\min}}$. With the new upper bound, p^{sf} still satisfies TSPD of order m with any thresholds $0 < \varepsilon_{\text{head}} \leq \frac{e^{-B}}{A_m}$, $\frac{(K - m)e^{-\gamma}}{\Omega_{\min}} \leq \varepsilon_{\text{tail}} \leq 1 - m \varepsilon_{\text{head}}$.

Proof. For any j , the softmax probability is given by:

$$p_j^{\text{sf}} = \frac{e^{-\delta_j}}{\Omega}, \quad \text{where } \Omega := 1 + \sum_{k \neq y} e^{-\delta_k}.$$

Based on the assumptions, the logit gaps satisfy:

- **Head** ($2 \leq k \leq m$): $\delta_{(k)} \leq B \implies e^{-B} \leq e^{-\delta_{(k)}} \leq 1$.
- **Tail** ($k > m$): $\delta_{(k)} \geq \gamma \implies e^{-\delta_{(k)}} \leq e^{-\gamma}$.

1. Lower bounds for the head candidates. To lower-bound p_y^{sf} and $p_{(k)}^{\text{sf}}$, we must upper-bound the partition function Ω . By taking the largest possible contributions from every token (setting $\delta_{(k)} = 0$ for the head and $\delta_{(k)} = \gamma$ for the tail), we obtain A_m :

$$\Omega \leq 1 + \sum_{k=2}^m 1 + \sum_{k>m} e^{-\gamma} = m + (K - m)e^{-\gamma} = A_m.$$

Therefore,

$$p_y^{\text{sf}} = \frac{1}{\Omega} \geq \frac{1}{A_m}, \quad p_{(k)}^{\text{sf}} = \frac{e^{-\delta_{(k)}}}{\Omega} \geq \frac{e^{-B}}{A_m} \quad (\forall k = 2, \dots, m).$$

2. Upper bound for the tail mass. The cumulated tail mass is given by:

$$T(\mathbf{z}) = \sum_{k>m} p_{(k)}^{\text{sf}} = \frac{\sum_{k>m} e^{-\delta_{(k)}}}{\Omega}.$$

To find the maximum tail mass, we must maximize the numerator and minimize the denominator. The numerator is maximized when tail gaps are minimal ($\delta_{(k)} = \gamma$). The denominator $\Omega = 1 + \sum_{k=2}^m e^{-\delta_{(k)}} + \sum_{k>m} e^{-\delta_{(k)}}$ is minimized when the head contributions are minimal ($\delta_{(k)} = B$). Let $\Omega_{\min} = 1 + (m-1)e^{-B} + (K-m)e^{-\gamma}$. Then:

$$\sum_{k>m} p_{(k)}^{\text{sf}} \leq \frac{(K-m)e^{-\gamma}}{\Omega_{\min}}.$$

This completes the proof of Remark 2. \square

Proposition 6 (Tightness of the Tail Bound). *Under the assumptions of Corollary 5, the upper bound on the softmax tail mass is tight.*

Proof. Consider the extremal configuration:

$$z_y = 0, \quad z_{(2)} = \dots = z_{(m)} = -B, \quad z_{(m+1)} = \dots = z_{(K)} = -\gamma.$$

This configuration satisfies all assumptions. The softmax tail mass becomes:

$$T_{\max}(K) = \frac{(K-m)e^{-\gamma}}{1 + (m-1)e^{-B} + (K-m)e^{-\gamma}}.$$

Let $a := e^{-\gamma}$, $b := 1 + (m-1)e^{-B}$, and $t := K-m$. We write $T_{\max}(K) = f(t) = \frac{at}{b+at}$. The derivative $f'(t) = \frac{ab}{(b+at)^2} > 0$ shows that the tail mass is strictly increasing in K . Moreover,

$$\lim_{K \rightarrow \infty} T_{\max}(K) = \lim_{t \rightarrow \infty} \frac{at}{b+at} = 1.$$

Thus, the maximum softmax tail mass can grow monotonically with K and approach 1, confirming the tightness of the bound.

E ADDITIONAL TECHNICAL ANALYSIS

E.1 A NEW TRAINING PARADIGM

Training with CE loss leads to distribution collapse: under gradient descent, the predictive distribution \mathbf{p} converges to the target y . This causes over-confident and degenerate predictions at inference.

To address this issue, we discuss a new paradigm consisting of three steps:

1. **Inflation during training.** Given $\mathbf{p}^{\text{sf}} = \text{softmax}(\mathbf{z})$, we define an inflated distribution

$$\tilde{p}_i = \frac{f(p_i^{\text{sf}})}{\sum_{j=1}^K f(p_j^{\text{sf}})}, \quad i = 1, 2, \dots, K,$$

where $f : [0, 1] \rightarrow \mathbb{R}_+$ is strictly increasing and satisfies a *ratio amplification* property:

$$p_i^{\text{sf}} > p_j^{\text{sf}} \implies \frac{f(p_i)}{f(p_j)} > \frac{p_i^{\text{sf}}}{p_j^{\text{sf}}}.$$

2. **Loss applied on the inflated distribution.** We train by minimizing a tailored loss $\ell(\tilde{\mathbf{p}}, y)$. Ratio-amplifying inflation accelerates the collapse of $\tilde{\mathbf{p}}$ to one-hot.

3. **Softmax inference.** At test time, predictions are made with the original \mathbf{p} , which remains smooth and calibrated.

This paradigm improves optimization dynamics while preserving smooth probabilistic predictions.

Theorem 7 (Invertible ϕ -mappings training prevents collapse at inference). *Given the predictive distribution \mathbf{p} , let ℓ be a strictly proper loss and $f : [0, 1] \rightarrow \mathbb{R}_+$ be strictly increasing and invertible. Define the inflated distribution*

$$\tilde{\mathbf{p}} = \Phi(\mathbf{p}), \quad \Phi(\mathbf{p})_i = \frac{f(p_i)}{\sum_{j=1}^K f(p_j)}$$

where $i = 1, 2, \dots, K$.

1350
1351 1. **(Training)** Under gradient descent, $\tilde{p}_y = 1$ when this loss converges to 0, i.e., the inflated
1352 distribution collapses to the one-hot label.

1353 2. **(Inference)** Define the recovered distribution

1354
1355
$$p_i^* = \frac{f^{-1}(\tilde{p}_i)}{\sum_{j=1}^K f^{-1}(\tilde{p}_j)}, i = 1, 2, \dots, K.$$

1356

1357 Then, \mathbf{p}^* remains strictly inside the simplex, that is
1358

1359
1360
$$\sum_{j=1}^K p_j^* = 1, \text{ and } 0 < p_j^* < 1 \forall j.$$

1361

1362 In particular, \mathbf{p}^* never collapses to a one-hot vector.
1363

1364 *Proof.* (1) For any strictly proper loss ℓ , the stationary condition
1365

1366
$$\nabla_{\mathbf{p}} \ell(\mathbf{p}, y) = 0 \iff p_y = 1$$

1367

1368 \implies the predictive distribution \mathbf{p} converges to the one-hot label. Since Φ is a bijection onto
1369 the simplex (as f is strictly increasing), minimizing $\ell(\Phi(\mathbf{p}), y)$ w.r.t. \mathbf{p} is equivalent to minimizing
1370 $\ell(\tilde{\mathbf{p}}, y)$ w.r.t. $\tilde{\mathbf{p}}$. Thus, under gradient descent in the inflated space, we obtain $\tilde{p}_y = 1$.

1371 (2) For inference, we recover \mathbf{p}^* from $\tilde{\mathbf{p}}$ via
1372

1373
1374
$$p_i^* = \frac{f^{-1}(\tilde{p}_i)}{\sum_{j=1}^K f^{-1}(\tilde{p}_j)}, \quad i = 1, 2, \dots, K.$$

1375

1376 Since $\tilde{\mathbf{p}} \in \Delta^{K-1}$, we have $0 \leq \tilde{p}_i \leq 1$ and $\sum_i \tilde{p}_i = 1$. Because f^{-1} is strictly increasing and
1377 continuous, we have $f^{-1}(\tilde{p}_i) \geq 0 \forall i$. Hence $p_i^* \geq 0 \forall i$, and normalization ensures $\sum_i p_i^* = 1$.

1378 To show non-collapse, suppose by contradiction that $p_y^* = 1$. Then $p_j^* = 0 \forall j \neq y$. But this would
1379 require $f^{-1}(\tilde{p}_j) = 0 \forall j \neq y$, i.e. $\tilde{p}_j = f(0)$. Since $\tilde{p}_j > 0$ (strictly inside the simplex), this is
1380 impossible. Thus \mathbf{p}^* cannot be a one-hot vector.

1381 Therefore, \mathbf{p}^* remains a smooth distribution in the simplex, preventing distribution collapse at inference. \square
1382
1383

1384 **Limit analysis.** Suppose $p_y = 1 - \epsilon$ with $\epsilon > 0$ distributed among other coordinates so that $p_j > 0$
1385 for some $j \neq y$. Then
1386

1387
$$\frac{\tilde{p}_y}{\tilde{p}_j} = \frac{f(1 - \epsilon)}{f(\epsilon)}.$$

1388

1389 Since f is strictly increasing and satisfies ratio amplification, we have
1390

1391
$$\lim_{\epsilon \rightarrow 0^+} \frac{f(1 - \epsilon)}{f(\epsilon)} = +\infty.$$

1392

1393 Therefore,
1394

1395
$$\lim_{\epsilon \rightarrow 0^+} \tilde{p}_y = 1, \quad \lim_{\epsilon \rightarrow 0^+} \tilde{p}_j = 0.$$

1396 In contrast, for the original distribution \mathbf{p} we only have
1397

1398
$$p_y = 1 - \epsilon < 1, \quad p_j = \epsilon > 0.$$

1399 Thus, the inflated distribution $\{\tilde{p}_i\}$ achieves the one-hot collapse strictly earlier, while the underlying
1400 \mathbf{p} remains smooth with strictly positive mass on all coordinates.
1401

1402 At inference time, we return to \mathbf{p} by applying the original activation function (e.g., softmax). This
1403 ensures the predicted distribution is smoother and less degenerate than one-hot, even though the
training dynamics in the inflated space enforced early collapse.

1404
 1405 **Theorem 8** (Sparsemax as a piecewise ratio-amplifying ϕ -mapping of softmax). *Let $\mathbf{z} \in \mathbb{R}^K$ be a
 1406 logit vector, $\mathbf{p}^{\text{sf}} = \text{softmax}(\mathbf{z}) \in \Delta^{K-1}$ with*
 1407

$$1408 \quad p_i^{\text{sf}} = \frac{e^{z_i}}{\sum_{j=1}^K e^{z_j}}, \quad i = 1, 2, \dots, K;$$

1409
 1410 and $\mathbf{p}^{\text{sp}} = \text{sparsemax}(\mathbf{z}) \in \Delta^{K-1}$ with
 1411

$$1412 \quad p_i^{\text{sp}} = \max\{z_i - \tau(\mathbf{z}), 0\}, \quad \sum_i p_i^{\text{sp}} = 1.$$

1413
 1414 *Then we define*
 1415

$$1416 \quad p_i^{\text{sp}} = \Phi(p)_i = \frac{f(p_i)}{\sum_{j=1}^K f(p_j)},$$

1417
 1418 where $f : [0, 1] \rightarrow \mathbb{R}_{\geq 0}$ is the piecewise function $f(x) = \max\{\log x - \theta, 0\}, \forall \theta \in \mathbb{R}$.
 1419

1420
 1421 *Proof.* According to $p_i^{\text{sf}} = \frac{e^{z_i}}{\sum_j e^{z_j}}$, we have $z_i = \log p_i^{\text{sf}} + C$ with $C = \log \sum_j e^{z_j}$. Substituting
 1422 this into the definition of sparsemax,
 1423

$$1424 \quad p_i^{\text{sp}} = \max\{\log p_i^{\text{sf}} + C - \tau(\mathbf{z}), 0\}.$$

1425
 1426 Letting $\theta = \tau(\mathbf{z}) - C$, we obtain

$$1427 \quad p_i^{\text{sp}} = \max\{\log p_i - \theta, 0\}.$$

1428
 1429 Since $\sum_i p_i^{\text{sp}} = 1$, normalizing yields
 1430

$$1431 \quad p_i^{\text{sp}} = \frac{\max\{\log p_i - \theta, 0\}}{\sum_j \max\{\log p_j - \theta, 0\}}.$$

1433
 1434 We now analyze the following two cases.

1435
 1436 *Case 1 (support set $S^{\text{sp}}(\mathbf{z}) = \{i : \log p_i^{\text{sf}} > \theta\}$).* For $i \in S$, $f(p_i^{\text{sf}}) = \log p_i^{\text{sf}} - \theta > 0$. On $(0, 1]$,
 1437 $\log x$ is strictly increasing; subtracting θ preserves this property. Therefore $\forall i, j \in S$ with $p_i^{\text{sf}} > p_j^{\text{sf}}$,
 1438 we obtain the ratio amplification property:

$$1439 \quad \frac{\Phi(\mathbf{p})_i}{\Phi(\mathbf{p})_j} = \frac{\log p_i^{\text{sf}} - \theta}{\log p_j^{\text{sf}} - \theta} > \frac{p_i^{\text{sf}}}{p_j^{\text{sf}}}.$$

1440
 1441 Thus Φ inflates the relative ratios within the support.

1442
 1443 *Case 2 (outside the support $S^{\text{sp}}(\mathbf{z})$).* For $j \notin S^{\text{sp}}(\mathbf{z})$, we have $\log p_j^{\text{sf}} \leq \theta$ and hence $f(p_j^{\text{sf}}) = 0$.
 1444 Therefore,

$$1445 \quad \Phi(\mathbf{p})_j = \frac{0}{\sum_{i \in S^{\text{sp}}(\mathbf{z})} f(p_i^{\text{sf}})} = 0.$$

1446
 1447 By contrast, $p_j^{\text{sf}} > 0$ since $\mathbf{p} = \text{softmax}(\mathbf{z})$ has full support. Thus $\text{sparsemax}(\mathbf{z})$ coincides with
 1448 $\Phi(\mathbf{p})$, where Φ is generated by the piecewise ratio-amplifying function f . \square
 1449

1450
 1451 Overall, sparsemax(\mathbf{z}) is a piecewise ratio-amplifying inflation of softmax(\mathbf{z}). Training on $\Phi(\mathbf{p})$
 1452 drives the inflated distribution to collapse to one-hot on its support, while inference with the original
 1453 softmax \mathbf{p} preserves strictly positive mass on all coordinates. This prevents the predictive distribution
 1454 from degenerating into an exact one-hot vector at inference.

1455
 1456 Having established sparsemax as a concrete instance of ratio-amplifying inflation, it is natural to
 1457 ask whether *other* mappings f might be equally effective, or perhaps even more suitable in specific
 contexts. To answer this, we next examine the general collapse condition in the binary case.

1458
1459

E.2 GENERAL COLLAPSE CONDITION IN THE BINARY CASE

1460

Consider binary classification with $\mathbf{p} = (p, 1 - p)$ and label $y = 1$. The inflated distribution is

1461

1462
$$\tilde{p}_1 = \frac{f(p)}{f(p) + f(1 - p)}, \quad \tilde{p}_2 = 1 - \tilde{p}_1.$$
1463

1464

Define the ratio

1465

1466
$$R(p) = \frac{f(1 - p)}{f(p)}.$$
1467

1468

Then

1469

1470
$$\tilde{p}_1 = \frac{1}{1 + R(p)}.$$
1471

1472

For a precision parameter $\epsilon > 0$, we say collapse occurs if

1473

1474
$$\tilde{p}_1 \geq 1 - \epsilon \iff R(p) \leq \frac{\epsilon}{1 - \epsilon}.$$
1475

1476

1. Power inflation. For $f(x) = x^\alpha, \alpha > 1$,

1477

1478
$$R(p) = \left(\frac{1 - p}{p}\right)^\alpha.$$
1479

1480

Collapse condition:

1481

1482
$$p > \frac{1}{1 + \left(\frac{\epsilon}{1 - \epsilon}\right)^{1/\alpha}}.$$
1483

1484

2. Exponential inflation. For $f(x) = e^{\gamma x}, \gamma > 0$,

1485

1486
$$R(p) = e^{\gamma(1 - 2p)}.$$
1487

1488

Collapse condition:

1489

1490
$$p > \frac{1}{2} + \frac{1}{2\gamma} \log \frac{1 - \epsilon}{\epsilon}.$$
1491

1492

3. Logarithmic inflation. For $f(x) = \log(x + \delta)$ with $\delta > 0$,

1493

1494
$$R(p) = \frac{\log(1 - p + \delta)}{\log(p + \delta)}.$$
1495

1496

Collapse condition:

1497

1498
$$\frac{\log(1 - p + \delta)}{\log(p + \delta)} < \frac{\epsilon}{1 - \epsilon}.$$
1499

1500

E.3 GRADIENT DYNAMICS UNDER RATIO AMPLIFICATION

1501

The ratio-amplifying property of ϕ -mappings not only accelerates the collapse of $\tilde{\mathbf{p}}$, but also reshapes the gradient dynamics during training. For a strictly proper loss ℓ , the gradient w.r.t. logits \mathbf{z} is assumed to be

1502

1503
$$\nabla_{\mathbf{z}} \ell(\mathbf{z}; y) = \mathbf{p} - \mathbf{e}_y, \quad \mathbf{p} = g(\mathbf{z}),$$
1504

1505

where $g(\cdot)$ denotes a probability distribution obtained from the logits \mathbf{z} and \mathbf{e}_y is a one-hot vector with the y -th entry equals 1.

1506

When training on the inflated distribution $\tilde{\mathbf{p}} = \Phi(\mathbf{p})$, the chain rule gives

1507

1508
$$\nabla_{\mathbf{z}} \ell(\tilde{\mathbf{p}}, y) = \frac{\partial \tilde{\mathbf{p}}}{\partial \mathbf{p}} \cdot (\tilde{\mathbf{p}} - y),$$
1509

1510

where $\frac{\partial \tilde{\mathbf{p}}}{\partial \mathbf{p}}$ is the Jacobian of the inflation operator.

1511

1512 **Effect of ratio amplification.** Suppose $f : [0, 1] \rightarrow \mathbb{R}_+$ is strictly increasing and ratio-amplifying,
 1513 so that

$$\frac{\tilde{p}_y}{\tilde{p}_j} > \frac{p_y}{p_j}, \quad \forall j \neq y.$$

1516 This guarantees that the *relative gap* between the correct and incorrect probabilities grows under Φ .
 1517 Hence, even if the exact magnitude of each gradient entry depends on the Jacobian structure, the
 1518 ratio

$$\frac{|\nabla_{z_y}|}{|\nabla_{z_j}|}$$

1521 is enlarged compared to the original probability space. In other words, the margin $z_y - z_j$ receives
 1522 stronger effective gradient pressure to grow. Intuitively, because $\tilde{p}_y > p_y$ and $\tilde{p}_j < p_j$ for $j \neq y$,
 1523 the gradient signal on the correct logit z_y is reinforced, while the signals on the incorrect logits z_j
 1524 are diminished. This rescaling accelerates the suppression of false classes and boosts the dominance
 1525 of the true class. Although the absolute gradient values are determined by both \tilde{p} and the Jacobian
 1526 $\frac{\partial \tilde{p}}{\partial p}$, the effective separation between correct and incorrect classes is consistently larger under ratio-
 1527 amplifying mappings.

1528 **Summary.** Any ϕ -mapping with ratio amplification reshapes the optimization dynamics by pre-
 1529 conditioning the gradient flow:

- The *relative strength* of gradients is tilted further in favor of the true class.
- Incorrect classes are suppressed earlier, as their probabilities are diminished more aggressively.

1535 Consequently, the system reaches effective one-hot collapse earlier than when training directly on p .
 1536 Crucially, since inference is carried out with the original distribution p , the final predictions remain
 1537 smooth and non-degenerate, preserving diversity while benefiting from sharper supervision during
 1538 training.

1539
 1540
 1541
 1542
 1543
 1544
 1545
 1546
 1547
 1548
 1549
 1550
 1551
 1552
 1553
 1554
 1555
 1556
 1557
 1558
 1559
 1560
 1561
 1562
 1563
 1564
 1565